(NASA-CR-147935) FURTHER LABORATORY STUDY OF THE DIFFUSE REFLECTANCE SPECTRA OF FROSTS OCCURRING ON ASTRONOMICAL OBJECTS Final Report (Pan American Univ., Edinburg, Tex.) 66 p HC $4.50 CSCL 20F G3/74

N76-23982

Unclas 28135

FINAL REPORT

FURTHER LABORATORY STUDY OF THE DIFFUSE REFLECTANCE SPECTRA OF FROSTS OCCURRING ON ASTRONOMICAL OBJECTS

by

Frederic M. Glaser
Pan American University
Edinburg, Texas 78539

prepared for:

NATIONAL AERONAUTICS AND SPACE ADMINISTRATION

Headquarters, Washington, D. C. 20546

May, 1976

Contract NGR 44-087-002 Supplement Number 1

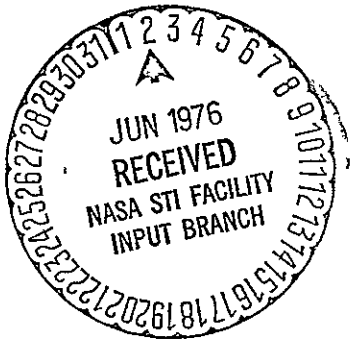

TABLE OF CONTENTS

ABSTRACT

Additions and changes to the apparatus include a residual gas analyzer, data logging system, rearrangement of the light collecting mirrors, improvements in the vacuum pumping system, and improved window sealing techniques. These changes have made a substantial improvement in how the system operates Pump oil contamination of the sample is shown not to be significant and the background vacuum has been brought into the 10^{-8} Torr range. At these low pressures the time required to accumulate a monolayer of condensable vapor becomes comparable to the experiment time and thus should not cause misleading absorptions. Even though the amount of light which can be brought to a detector has been increased by repositioning the mirrors, insufficient detector sensitivity continues to be a problem at both long and short wavelengths.

Two mineral samples, oligoclase and bloedite, have been investigated, and the diffuse reflectance spectra are presented. These data are for powdered material, 50μ to 5μ size mixture, cooled to 160°K The reflectivity of the oligoclase sample was also measured at room temperature, about 290°K, and the results at these two temperatures do indicate some tentative differences.

A frost of ordinary water was prepared and its spectral reflectance is presented. This result compares reasonably well with measurements made by other investigators.

Improvements in Instrumentation

The sample preparation chamber has been changed slightly in its mechanical layout to improve the optical transmission of the system. Previously, the two light collecting mirrors were supported vertically from the inside bottom of the chamber. Once they were fixed and the system evacuated, it was not possible to change their position or to rotate them. They had to be aligned as well as possible before the upper flange was in place and pumping began. In spite of our best efforts, this procedure was not very satisfactory and was time consuming. These elements are now supported through the upper flange by rotary shaft vacuum seals. Although no movement in the horizontal plane is possible once the system is closed, vertical and rotational motions can be effected. The amount of light collected from the sample and the standard is determined in part by the angular position of these mirrors. Because the sample is approximately five millimeters behind the plane of the standard, this difference in geometry causes the light collecting mirror to focus at a different position for the standard and the sample. Most of this inequality can be removed by rotating the mirrow about a vertical axis and the difference in image size and position is corrected during data analysis. This correction is made by comparing the radiation received from the standard reflector when it is in its usual position with the amount

of radiation received when it occupies the sample's position. The correction is less than two percent when the mirror is rotated to bring the detector response to a maximum. Since only about ten percent or less of the monochromator output energy is brought to the detector, it is advantageous to present the sample and detector with the maximum energy available in order to reduce the effects of noise, etc. The change in the mirror mounting has made a significant increase in the optical through-put of the system.

The achievable vacuum in the sample preparation chamber has been improved significantly by incorporating several modifications into the system. The lowest pressure attained previously was about 3×10^{-6} Torr and excessive outgassing was proposed as the most likely cause of the inability to reach lower pressures. Several changes and improvements have been made so that initial pressures in the 5×10^{-8} Torr range are reached with only a modest effort. Some welds were reworked, all O-ring seals are made using Viton A O-rings, a Freon refrigerated baffle replaced the water cooled one between the diffusion pump and the liquid nitrogen trap, and DC-705 fluid is used in the vapor pump. Pressures in the 10^{-8} range can be achieved after pumping for twelve to eighteen hours with warming to around 75°C. It was observed that although the system tested leak-free when pumping was initiated, one or more windows usually developed a leak sometime during the experiment The windows were cemented into aluminum flanges using a vacuum grade of epoxy resin (Ve-Seal).

Apparently the differential thermal expansion of the aluminum and window material exceeded the cement's ability to deform sufficiently to maintain a vacuum tight seal. Aging also appeared to be involved. All these cemented windows have been replaced with ones making the vacuum seal by forcing the window against an O-ring with a hollow, externally threaded piece. The 20mm window pieces had to be replaced with pieces of 38mm diameter to accommodate the 14mm slit height using an O-ring and forcing piece. This change has eliminated a major source of frustration and delay. There are three window materials set in appropriate flanges, LiF, fused quartz, and KRS-5. By interchanging these on the entrance port, the reflectance from 1050Å to 35 microns can be measured

A Varian residual gas analyzer, Model VGA-100, has been connected to the sample preparation chamber. This instrument can be used as a leak detector as well as a mass spectrometer. This spectrometer has operated nicely, except that the RF-source had to be replaced when it developed an arc somewhere in the sweep voltage circuit. Varian replaced the defective unit but much effort was expended learning to properly tune the quadrapole analyzer. The unit performs well now and hopefully no further difficulties will be encountered.

The prime function of the gas analyzer is to monitor the cleanliness of the sample environment. This RGA instrument is capable of detecting partial pressures on the order of 2×10^{-11} Torr. Figure 1 is a typical mass spectrum showing the relative amounts of residual gas. The system pressure was

about 8×10^{-8} Torr, which was achieved after pumping overnight with warming to 75°C. The spectrum shows that water is the dominant constituent at a partial pressure of approximately 3×10^{-8} Torr. After several days of pumping on the heated system, the base pressure can be reduced to about 3×10^{-8} Torr, and virtually all the water, methyl alcohol, and acetone are removed, nitrogen and carbon dioxide are the principal constituents remaining.

The important point shown by this mass spectrum is that material in the 60 to 100 amu range is present at pressures of less than 1×10^{-10} Torr. Material with these masses can be derived from mechanical pump oil. The mechanical pump is trapped with Linde molecular sieve to prevent backstreaming. There are other sources of oil as well, such as O-rings, unremoved fingerprints, and oil mist in the air from pumps and motors, which all contribute to the problem of possible oil contamination. Assuming that the organics in the 60 to 100 amu and above are present at a pressure of about 1×10^{-10} Torr, a monolayer will form in about ten hours and, thus, will not interfere with the measurements. As a further test to detect possible oil contamination, the spectral reflectance of the clean, cooled (77°K) copper substrate was measured at 1216 A. The sample holder was orientated so that the reflected beam exited through the photography port and struck a sodium salicylate film. The fluorescence of this material was measured and the experiment carried out for over four hours. These data do not indicate any systematic reduction in

reflectance which would indicate the formation of an oil film. Small, random fluctuations due to changes in lamp output flux, detector response, noise, etc., were observed, but these were not different from what are normal for this apparatus. Thus, it appears that there will be little or no oil contamination of frost samples or cooled mineral samples during the reflectance measurements. The residual gas can be analyzed occasionally during the experiment to check for high molecular weight materials, but the instrument cannot be taking gas analysis data while the photometric measurements are being made because of the ionizer's filament emission.

A data acquisition system has been put into operation so that the data reduction and analysis can be performed by the University computer. The system is composed of a scanner, digital voltmeter and paper tape punch with controller. The scanner can take up to ten channels of analog input, switching each of these to the voltmeter for conversion to digital form. Dwell times ranging from 10 sec to 6 ms are available plus a manual mode of channel changing. By using different speed motors on the wavelength drive of the monochromator, a wide range of sampling rates is available. Which of these sampling rates is used in taking data is dictated by a variety of factors, such as response speed and noise of the radiation detector, monochromator slit width, grating used, and so on, the whole range has been used at various times. The voltages are measured by the voltmeter and are converted from an analog representation to serial binary coded decimal (BCD) format.

The voltmeter is a 5½ digit autoranging instrument capable of resolving 0.1 mV. The voltages of concern here lie between 0v and about 2.5v which includes two ranges of the voltmeter. Some difficulty has been encountered with the ±5v logic power supply of this instrument. Hopefully, this has been corrected so that further data collecting can proceed at a rapid pace.

The digital output from the voltmeter together with the channel number is sent to the punch controller which then activates the paper tape punch. The data is placed on the paper tape in ASCII format to be read and processed later. At present, the lengths of paper tape are taken to the University computer center where they are read on to disk storage. This is done by computer center personnel as time and the job load permits. Eventually, these records are processed to form the desired result the reflectance of the sample as compared to the standard as a function of wavelength. The intensity data from several runs are combined and statistical significance of deviation from the average can be computed. This information is recorded on magnetic tape as well as the raw data. The results are presented both in tabular form and as a plot of intensity ratio versus wavelength together with the calculated standard deviation in the intensity ratio. The results are presented in this form in a following section.

A further improvement in the operating system should be pointed out. Although Pan American University is located in a semi-arid region of Texas, it is near the Gulf Coast so that high humidity accompanies the prevailing southeast breeze.

During the night the humidity may be 90% or more, and it has been University policy not to air condition the classroom buildings beyond normal school hours. The resulting condensation and high humidity brought this project to a stop until the University made arrangements to air condition the laboratory continuously. A separate cooling and heating unit is now being installed in the laboratory which will provide a suitable environment for this apparatus independent from the rest of the building. The problems with high humidity, such as fogging of KBr and NaCl windows and leaking capacitors, should now be over. The malfunction of the RF unit for the residual gas analyzer and the ±5 volt power supply in the digital voltmeter are probably traceable to the humidity even though care was exercised not to operate these with visible condensation in the laboratory.

Difficulties and Problems Encountered

As will be seen from the results presented in the following section, no reliable reflectance data has been collected using radiation with wavelength shorter than 0.18μ. Further, no results are available in the infrared region beyond 2.5μ. Lack of sufficiently sensitive detectors has been the problem with obtaining accurate data in these regions.

A freshly prepared film of sodium salicylate is used as the fluorescent material to detect radiation in the far ultraviolet region. A quartz window is lightly coated with sodium salicylate by spraying the warmed window with a saturated solution of the salt in methanol. This fluorescence is viewed by an EMI 9783B photomultiplier tube. A low pressure hydrogen discharge has been used to provide the light in the 0.16μ to 0.10μ region. This spectrum consists of the molecular hydrogen emission bands and strong lines due to atomic hydrogen. When the vacuum monochromator is adjusted to pass the zero order spectrum on to the barium sulfate standard reflector, a reasonably strong signal of about 50 na is recorded using 25μ slits When the first order spectrum is swept across the standard, only the radiation near the 1608Å, 1578Å, and 1216Å lines are clearly distinguishable from the background. The photomultiplier tube is operated at an overall sensitivity of 200 amperes per lumen with a dark current

of 5.1 na. This dark current can be cancelled out using the adjustments of the picoammeter, but the residual fluctuations, being AC in nature, cannot be removed. These random fluctuations are usually less than 100 pa peaks when no radiation is allowed to fall on the photocathode. The maximum detected radiation produces a photocurrent of less than 1 na at Lyman α. The barium sulfate standard is probably absorbing most of the far UV radiation; efforts are being made to locate a more suitable material. A gold coated flat mirror can be substituted for the barium sulfate standard and then the far ultraviolet data "normalized" at some overlapping wavelength around 0.18μ to 0.16μ to that taken using the barium sulfate standard. The gold mirror would give primarily specular reflection of the far UV and little or no diffuse reflection.

Choosing a suitable infrared detector has been a very frustrating and disappointing experience. The Department had an old thermocouple detector which was returned to the factory and rejuvenated. This detector has a sensitivity of approximately 25 V/W. Although this detector is suitable for transmission work, the low levels of reflected radiation produce a signal which is completely lost in the inherent noise of this detector. A pyroelectric detector was then obtained to replace the thermocouple. This new detector has a triglycine sulfate (TGS) flake as the active element and has a measured sensitivity of 3039V/W and a N.E.P. equal to 1.4×10^{-10}W. The light detection system used in the infrared beyond 0.7μ is based on the synchronous detection of the

chopped light beam. The radiation is chopped at 13Hz with the detector signal and reference fed to a lock-in amplifier which indicates the magnitude of the detector response. A Nernst filament is used as the infrared radiation source and a germanium filter passes radiation from about 1.8μ to 20μ. When the monochromator is set to pass the zero order spectrum, pyroelectric detector response is about 100μV when the radiation is allowed to fall on the standard reflector. This signal is well above the noise level, however, when the first order dispersed spectrum is scanned, the maximum response of the detector is only a few tenths of a microvolt, less than 0.3μV, peaked around 2.0μ In spite of the extremely narrow band width the lock-in amplifier accepts, approximately .0025Hz, this signal is not very reproducible due to the noise. Two examples of data taken from the standard are shown in Figure 2. It is difficult to obtain meaningful intensity ratios at such low signal levels.

A lead sulfide detector has been used at room temperature to obtain data in the range from 1.1μ to 2.6μ and a S-1 response photomultiplier tube in the 0.7μ to 1.1μ region. The PbS detector works well and has a good response, although the sensitivity and NEP are not known. The infrared sensitive photomultiplier is somewhat noisy, since it is not cooled to reduce the photocathode dark current.

Two final difficulties should also be mentioned. The University DEC-10 computer is supposed to be a do-all machine for everyone, and, as such, it operates most of the time as

a time-shared system. Apparently some users are more equal than others, accounting and the library, for instance, and at times it has been difficult to obtain machine time to process the data. During certain runs it would have been helpful to see the results soon after the data was taken. The experiment could have been directed toward gathering more data in the most interesting regions or filling in portions where a very noisy signal made interpretation difficult. With machine time on a catch-as-catch-can basis, several days usually pass before the data is reduced, long after the experiment is over

The reflectance spectra of frosts and minerals is strongly influenced by the crystal morphology of the sample. Provision was made to photograph the sample and several were photographed. No really satisfactory pictures were made in which more than qualitative estimates of grain size could be made. The mineral samples were observed under the microscope, and the average grain size was estimated using standard geologic techniques. The grain size estimates for the frosts are simple qualitative guesses.

Reflectance Spectra of Frosts and Minerals

The diffuse reflectance spectra of two minerals, oligoclase and bloedite, and water frost are presented in Figures 4 to 11. Figures 4 to 7 are the raw results on an expanded wavelength scale and in segments just as it was collected. Each wavelength segment was obtained using a particular combination of radiation source, grating, slits, filter, and detector. The sample was the same for all spectral data collected from that material, i.e., the water frost spectra were all obtained from a single frost sample. In this manner effects of crystal morphology, thermal history, etc., are identical in all data for that sample of material.

The raw results presented in Figures 4 to 7 were graphically averaged to remove the noise and compressed into the wavelength scales presented in Figures 8 to 11. The standard deviation of the reflected intensity is available for the standard reflector and sample reflectance data. The standard deviation of the intensity ratio can be calculated from these data and representative values are included in the composite graphs. Generally, the observed standard deviation of the intensity ratios is about 0.05 except in the near infrared region, 0.7μ to 1.2μ where it is 0.10 or more. This portion tends to be less precise because of the noise characteristics of the photomultiplier tube used as an uncooled detector.

The mineral samples were obtained from Ward's Natural

Science Establishment and reduced to a fine powder by hand grinding in alumina mortars. No iron particles or other contamination of the mineral samples occurred by using such techniques. The water for the frost sample was double distilled from an all glass system and boiled vigorously before use to remove the dissolved gases. No further purification procedures were employed to try to remove the last traces of carbon dioxide, ammonia, and other gases from the water

The mineral powders were placed in the copper holder and compressed tightly with a small hand arbor press. Since the sample is orientated vertically, it must be packed tightly enough to remain in the holder. The barium sulfate powder is contained in a similar holder by compressing it in a similar manner. The sample thickness was about 3 mm after packing, the standard reflector thickness was also about 3mm. Previous studies of mineral reflectance spectra showed that different methods of sample preparation can cause differences in the absolute intensity, but does not significantly alter the intense spectral features. As the grain size of the mineral powder decreases the overall reflectivity usually increases. The weak spectral features generally are lost in this high reflectance, and the relative intensity of the stronger absorptions is much reduced. Only the most intense bands remain unaltered The positions of the bands remain unchanged in all cases, but their contrast does depend on the grain size to varying degrees. Water frost was formed until a thick layer, approximately 3 mm, as judged by direct

viewing, resulted. No interference from the copper sample holder should be encountered while using samples this thick. Previously, the reflectance of water and carbon dioxide frost showed that for thin samples the substrate exerted a major influence on the observed spectra, but for thicknesses greater than about 1.5 mm the frost samples were completely opaque. Several attempts to photograph these mineral samples and frosts produced unsatisfactory results. Little detail of the sample was recorded on film yet the grains were distinguishable with the naked eye. None of the photographs are included since they contain so little information.

Briefly, the technique used to obtain these results was to measure the reflected intensity from a standard material, Eastman White Reflectance Standard, as a function of wavelength and then repeat the measurements taking intensity data from the sample. Several scans were made alternating between the sample and standard; usually three to five scans were made on the sample as well as the standard. The data for each was then averaged, the ratio calculated, and the standard deviations determined and the results plotted as shown in the figures. In nearly all cases the wavelength segments overlap with the preceding and following segments, however, occasionally this is not the case because either the data was inadvertently omitted or it was of such poor quality as not to warrant inclusion. Near the ends of some wavelength segments, the filter bandpass characteristics or detector response make it difficult to achieve reasonably noise free signals. This is

most noticeable near 0.18μ, 0.8μ and 1.2μ, where the effects of noise, drift, and other instabilities are readily apparent. No effort was made to smooth these results, the results presented in Figures 8 to 11 do represent the "best fit" of the data. The standard deviation at various wavelengths is indidated by the error bars attached to the graph.

Oligoclase, Norway.

This mineral sample was obtained as small lumps which showed very pale yellow markings on an off-white (gray) background. The material was easily ground to a fine white powder of grain size in the 5μ to 30μ size. A 3 mm layer was packed into the sample holder and the system evacuated to a pressure of $2x10^{-7}$ Torr. The reflectance spectra was determined with the sample at room temperature (295°K) and at 160°K. These results are shown in Figures 4 and 5. There are no strong absorption features in the room temperature spectrum anywhere in the range presented, from .2μ to 2.5μ. In general, this mineral sample reflects about 80% of the incident light in the visible and near-infrared region. A general decline in reflectivity for wavelengths beyond 1.8μ is observed.

Although there are no strong absorption bands in the spectra of oligoclase at room temperature, there are features which can be identified with specific sources. The pale yellow streaks in the sample suggest iron as an impurity. The broad absorptions near 0 78 and 0.93 are indicative of

iron, but the characteristic ferric iron band near 0.7μ is not evident nor does the reflectance seem to decrease shortward of 0.5μ. Ferrous iron has a band near 1.0μ to 1.1μ, usually, and there seems to be an indication of an absorption near 1.1μ but this occurs right at the end of the photomultiplier's response characteristic and thus is not a very firm identification because of the poor S/N in this region. The increasing absorption beyond 1.8μ with band structure at 1.4μ, 2.2μ and 2.5μ all show that water is present in or on the mineral sample. Since the sample was observed at room temperature and in an evacuated chamber, there is little possibility of surface water occurring on the sample, such as dew or an adsorbed surface layer. Adsorbed water on the surfaces of the mineral grains would be observed, but these absorption features in the room temperature spectrum are probably due to water in the mineral structure itself. Water of hydration will render the usual strong free water bands as will water which is trapped in interstices of the mineral structure. This silicate mineral probably does not contain water of hydration but rather inclusions bearing fluid water.

When the mineral sample was cooled to 160°K, the reflection spectrum reveals several features which are more prominent as compared to the room temperature spectrum. The overall reflectance remains high, about 80%, but now the decreased reflectance in the blue and near ultraviolet region is evident. The broad, shallow absorptions at 0.76μ, 0.78μ, and 0.81μ are due to ferrous iron, but still there is

no strong evidence of the 1.0μ ferrous band. The band at 0 93μ may have shifted slightly to near 0.89μ, but this is very tentative, since this is the high noise region. The OH stretching band at 1.38μ is the most distinguishing feature in the spectrum. Both free water and OH exhibit this band with water showing additional bands near 1.9μ. Unfortunately the spectrum of the cooled oligoclase sample does not extend beyond 1.6μ because detector problems were encountered and the experiment had to be discontinued before this data was taken. Since the same sample at room temperature has several bands attributed to water which appear in the region beyond 1.8μ, the 1 38μ band is due to water. This water is held as fluid (solid at low temperatures) at inclusions in the mineral structure.

Bloedite, California.

The sample of bloedite was received as a large crystal which was black when viewed in reflection, but was transparent when viewed in transmission. The source of the color was a black material distributed throughout the crystal in an uneven manner so that clear lines of sight were possible. No direct attempt to identify this black material has been made, but the spectrum indicates the presence of ferric iron, so that hematite is a good candidate. When a portion of this mineral was reduced to a fine powder, it became pure white in external appearance with small flecks of black material. The particle sizes of the ground material lie in the 75μ to 5μ range.

Only the low temperature spectrum of bloedite is presented. It shows a high overall reflectivity, 70-80%, with several distinct bands. The presence of water is demonstrated by the bands at 1.9μ, 1.75μ, and 1.36μ with the other band probably a combination of the OH stretching modes with lattice vibrations or a librational mode of water. The shallow bands at 0.70μ and 0.78μ are due to ferric iron as is the gradual decrease in reflectivity in the blue and near ultraviolet end of the spectrum. There are other broad, shallow features in the visible and near ultraviolet which are probably due to the iron also.

Water Frost.

The water frost was formed by vapor deposition on the cooled copper substrate. The frost was fine grained but no quantitative size can be given. The layer was grown until it was several millimeters thick; it was estimated to be about 3 mm by direct visual observation. The frost was deposited very slowly, about six hours were required, and the temperature of the substrate remained at 160°K ±1°K during the entire experiment. If the deposition rate is sufficiently slow, the heat of sublimation can be conducted away rapidly enough so that the surface temperature of the frost will not be far different from the substrate temperature. It is well known that water can crystallize in several different forms at low temperatures and pressures, however, by controlling the temperature and deposition rate closely, it is believed

that only one form of ice was produced, namely, hexagonal ice.

The reflectance spectrum of water ice resembles that of the vapor and is well known in the spectral region investigated here. The ice absorbs strongly in the ultraviolet shortward of 0.21μ falling to near zero reflectance at 0.18μ. The absolute reflectance in just this region is very uncertain for this is where the Schumann-Runge bands of molecular oxygen appear. Although the monochromator, source, and detector were continually purged with dry nitrogen, these oxygen bands persisted in the spectra. A previously reported feature at 0.195μ in the reflectance spectra of hexagonal ice is not seen, but due to the strong oxygen band, it may be merely obscured.

The reflectance of this water ice is featureless from about 0.21μ to 0.8μ with the reflectivity being in the 80% to 90% range. The decline in reflectivity from 0.32μ to 0.36μ is probably not real, but rather degraded detector performance is probably the cause of this decline. Again, the region from 0.65μ to 0.77μ is extremely noisy due to the noise in the uncooled S-1 photomultiplier tube. A severe loss of data due to this problem is seen in the region from 0.8μ to 1.2μ where essentially complete loss of signal occurred. When the lead sulfide detector was used in the 1.3μ to 1.9μ range, the sharp absorption peak at 1.4μ is easily seen and the broad strong absorption centered at about 1.6μ is clearly evident. The reflectance increases beyond 1.7μ before the

indication of absorption at 1.9μ is seen.

The spectrum of oligoclase powder in the spectral region from 0.3μ to 2.5μ taken at room temperature has been available for some time. The reflectance of water frost from 0.17μ to 12μ at a variety of temperatures and conditions, some known and others unspecified, has also been presented previously. The reflectance spectrum of bloedite is not so well known and the spectra of minerals at low temperatures as expected on satellite and asteroid surfaces have not been measured. In this sense the, these mineral data are new results.

A tentative comparison of the effect that cooling the mineral has on the spectra can be made from the two spectra of oligoclase. This soda feldspar sample shows iron as a trace element and water which is probably held as inclusions. The room temperature spectra shows two weak bands at 1.5μ and 0.93μ with a very weak absorption at about 0.78μ. The 1.5μ band probably is a water band that has been displaced slightly. The spectra taken of the cooled sample again shows two weak absorptions, but they are much sharper and the water band at 1.38μ is unmistakable. The band at 0.93μ is no longer evident, but the iron band at 0.78μ is also quite sharp. The cooled sample shows a distinct decrease in reflectivity on going to shorter wavelengths. This trend is evident starting from about 0.5μ until the absorption edge at 0.21μ is encountered. Some indications of absorptions at 0.35μ and 0.25μ appear but these are not very well

established. In contrast the visible and near ultraviolet reflectance of the sample at room temperature remains near 70% down to 0.2μ with perhaps a very broad feature around 0.25μ. A simple conclusion can be drawn in that although no major changes in the spectra of this mineral appear when it is cooled to 160°K, the spectra has a temperature dependence. The extent of this behavior remains to be explored and many more mineral examples should be investigated.

There remains one nagging question concerning the validity of this comparison. Could the water features seen in the spectra of the cooled mineral be due to frost on the surface? One must reply in the affirmative that water could have condensed on the sample surface causing the characteristic features. However, there is evidence that this is not the cause of these features. The spectra of water frost shows the absorption edge at 0.2μ and a sharp band at 1.4μ which are observed in the cooled oligoclase result. In addition to these features, water frost has a very strong, broad band centered near 1.5μ to 1.6μ and another broad feature centered around 1.2μ to 1.3μ These two bands are well known in the water frost spectrum and are unmistakable. No sign of the absorptions are seen in the cooled sample spectrum nor in the spectrum taken at room temperature. The spectrum of cooled bloedite shows the 1.4μ water band but not the strong broad 1.2μ and 1.6μ bands characteristic of water frost. Further, the reflectance of cooled bloedite remains moderately high to below 0.2μ with no indication of

an absorption edge at this wavelength. Finally, since the samples were placed in a good vacuum in which the partial pressure of water was probably in the 10^{-8} Torr range, there simply wasn't much water in the system to condense. The data taking extended over several days so that even at very low water vapor pressures it is possible that a thin film of condensate could have formed. This possibility will be investigated thoroughly before a definite statement can rule out the formation of an extraneous frost deposit interfering with these measurements

Further Improvements and Projections

Several deficiencies in the experimental techniques employed in the data gathering system have been pointed out and the results presented have made clear several areas where improvements are necessary. Shortened turn-around time in the data reduction and processing tasks would be helpful in eliminating the gaps in spectra caused by excessive noise, low signal ratios, etc., as encountered in the near infrared portion of the water frost spectrum. To this end the Department expects to receive a grant to purchase a minicomputer to be used in new course work and to be available for Departmental research. It may be possible to interface the data acquisition system directly to this computer to give nearly real time data analysis. In any event, this machine will be available to process data from this project, and since the operation of the machine will be the responsibility of this author, much better turn-around time will be experienced. Another problem which will be resolved shortly is that of determining grain size of the frost in situ. Better photography skills are being developed which should improve the quality of the graphic records of the frosts. Also a measuring telescope with a calibrated reticle will be procured. This instrument will permit a better estimate of the grain size and can, perhaps, be adapted to provide telescopic photography of the sample.

The difficulty with light intensities which are reliably detected is being worked on from both the radiation

source and detector ends of the optical train. In the far ultraviolet region, the sodium salicylate covered window is to be replaced with a solar blind photomultiplier tube which will mate directly to an experiment chamber port. This detector tube has a magnesium fluoride window and a cesium iodide photocathode, thus, it is sensitive to radiation in the 0.11μ to 0.20μ range. The dark current is rated at less than 10 pa at a gain of 10^6. The increased sensitivity in this region provided by the tube may negate the necessity of locating an alternative diffuse reflectance standard. To further increase the ability to make reliable measurements in this short wavelength region, a condensed spark discharge power supply is being designed to function at a total output power of about 1kW. This source is the well-known thyratron trigger circuit. This power supply should increase the available radiation and make a better signal to noise ratio possible.

At the other end of the spectrum, a dry-ice cooled chamber for the infrared sensitive photomultiplier tube should eliminate most of the noise encountered in the near infrared region. For radiation beyond 2.5μ, a much more sensitive detector is required than the pyroelectric detector now being used. One of the most sensitive infrared detectors made is the cooled germanium bolometer. When cooled to liquid helium temperatures or lower, these elements exhibit detectivities on the order of 10^{-14}watt/$\sqrt{\text{Hz}}$. One of these detectors has been ordered together with the appropriate

cryostat, window and other accessories. This detector should alleviate the problems due to the lack of sufficient sensitivity to make trustworthy measurements beyond 2.5μ.

Another step to improve the optical performance of the instrument may be necessary, namely, complete removal of the atmosphere from the system. At present, the experiment chamber and detector are evacuated when the measurements are made while the monochromator is purged with dry nitrogen. There is no provision for placing the radiation source in an atmosphere free condition. Thus, there are a few decimeters of optical path in ordinary atmosphere which provide all of the usual water vapor, carbon dioxide, etc., absorptions. These bands do not interfere strongly in the near infrared because of the short path length, but provision for operating the source in an atmosphere free of these absorbers will be necessary if reliable data is to be obtained at longer wavelengths. Several ideas for running the sources in such a condition are under consideration. One option for future consideration is to eliminate any atmosphere completely, i.e., turn to a vacuum infrared system.

ACKNOWLEDGEMENTS

I wish to acknowledge the assistance and suggestions made by Drs. F. P. Fanale, D. L. Matson, T. V. Johnson and L. Lebofsky at the Jet Propulsion Laboratory, Pasadena, California. The assistance of Sandy Richardson, Ricardo Cantu, and Paul Killam of Pan American University is gratefully acknowledged. I also wish to thank John Hook, Vice President of Pan American University, for arranging for the continuous air conditioning of the laboratory space.

FIGURE CAPTIONS

Figure 1. Typical mass spectrum of residual gas in the experiment chamber at a total pressure of 8×10^{-8} Torr.

Figure 2. The far ultraviolet emission spectrum of H_2 after reflection by the diffuse reflectance standard.

Figure 3. The signal from the pyroelectric IR detector operating in the near IR. The signal is derived from the reflected radiation from a Nernst filament off the standard reflector.

Figure 4 a-g. The reflectivity of Oligoclase powder (50μ to 5μ sizes) at 290°K.

Figure 5 a-g. The reflectivity of Oligoclase powder (50μ to 5μ sizes) at 160°K.

Figure 6 a-f. The reflectivity of Bloedite powder (75μ to 5μ) at 160°K.

Figure 7 a-f. The reflectivity of Water frost at 160°K.

Figure 8 a,b. Reflectivity of Oligoclase powder at 290°K.

Figure 9 a,b. Reflectivity of Oligoclase powder at 160°K.

Figure 10a,b. Reflectivity of Bloedite powder at 160°K.

Figure 11a,b. Reflectivity of Water frost at 160°K.

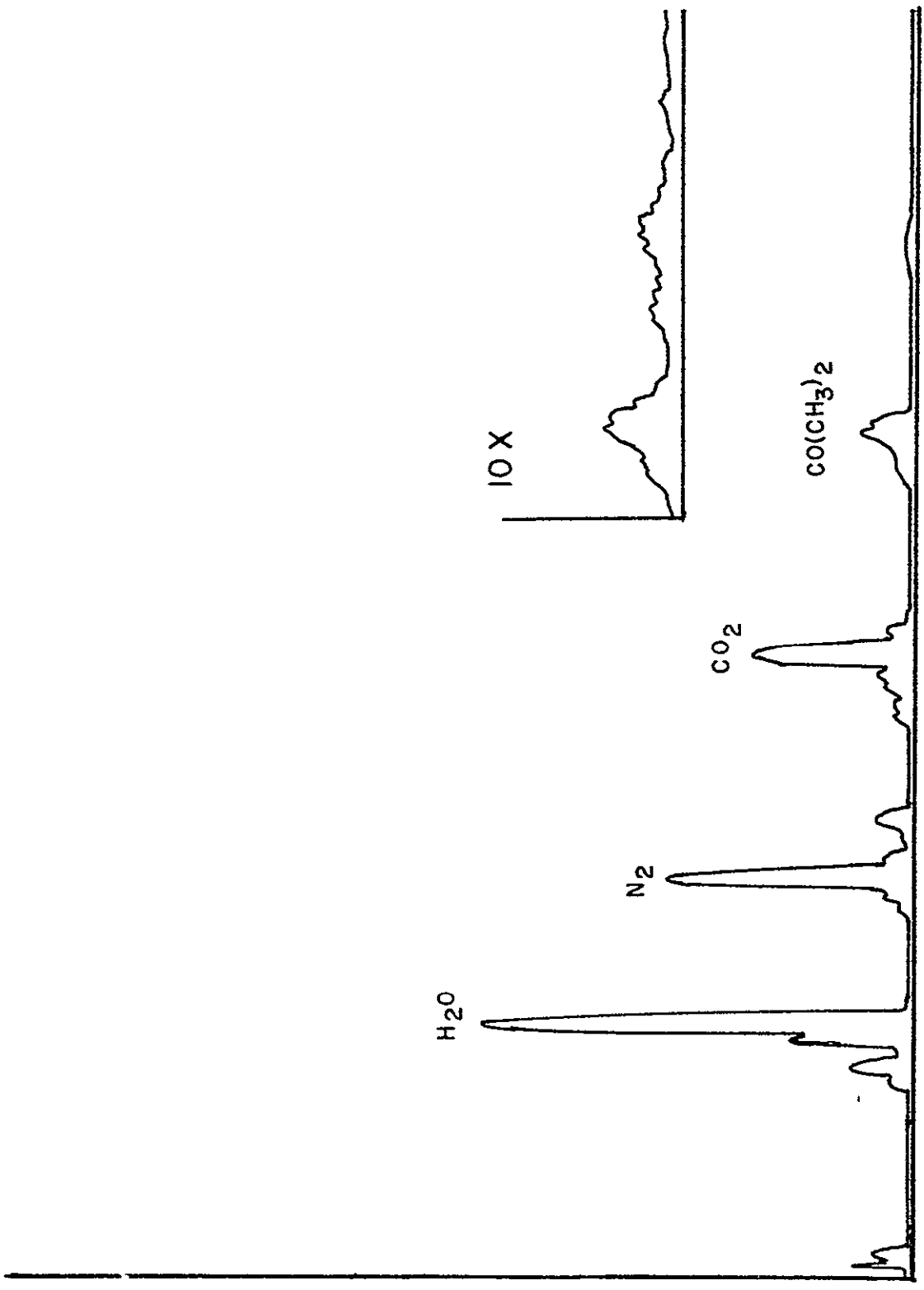

FIG. 1

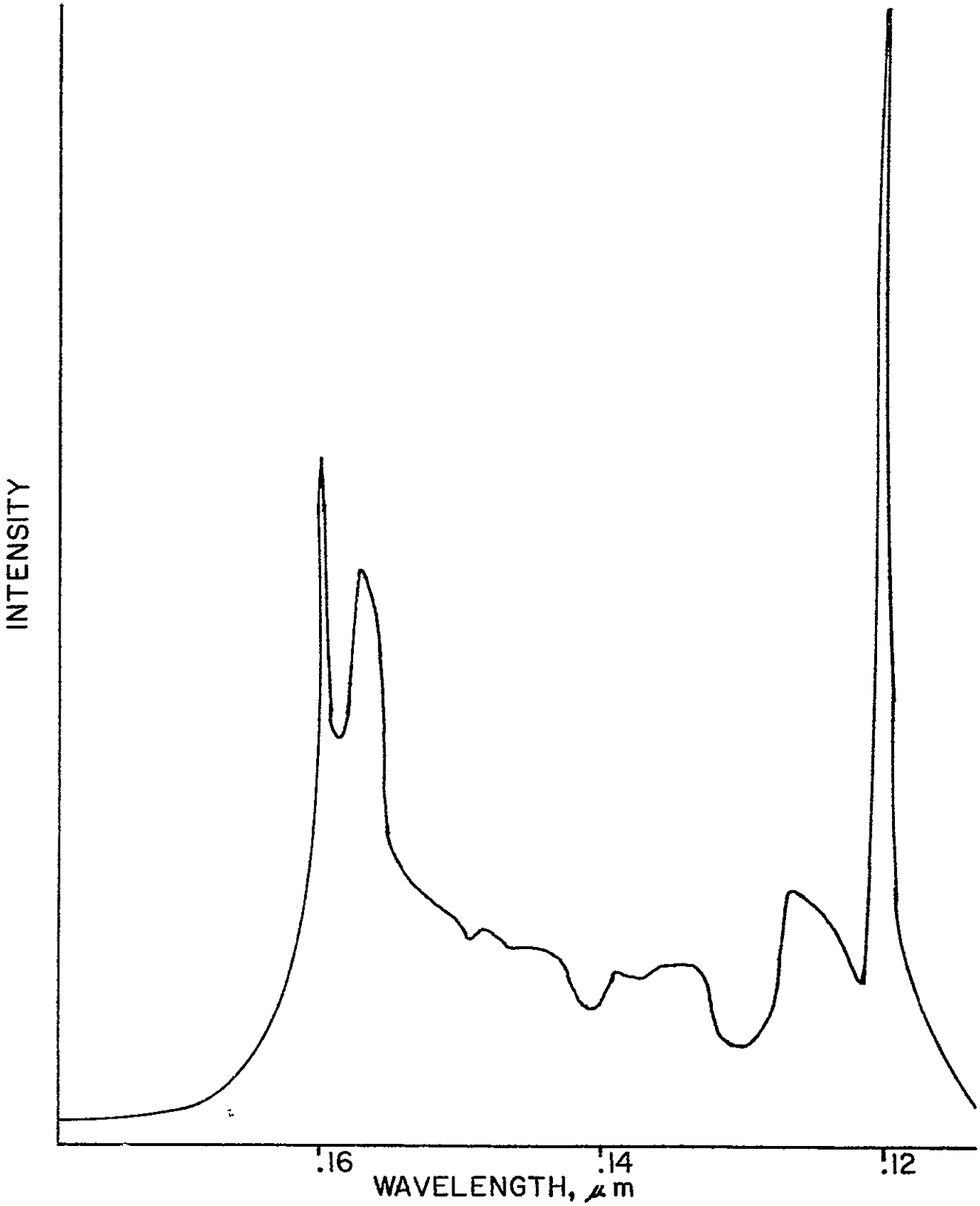

FIG. 2

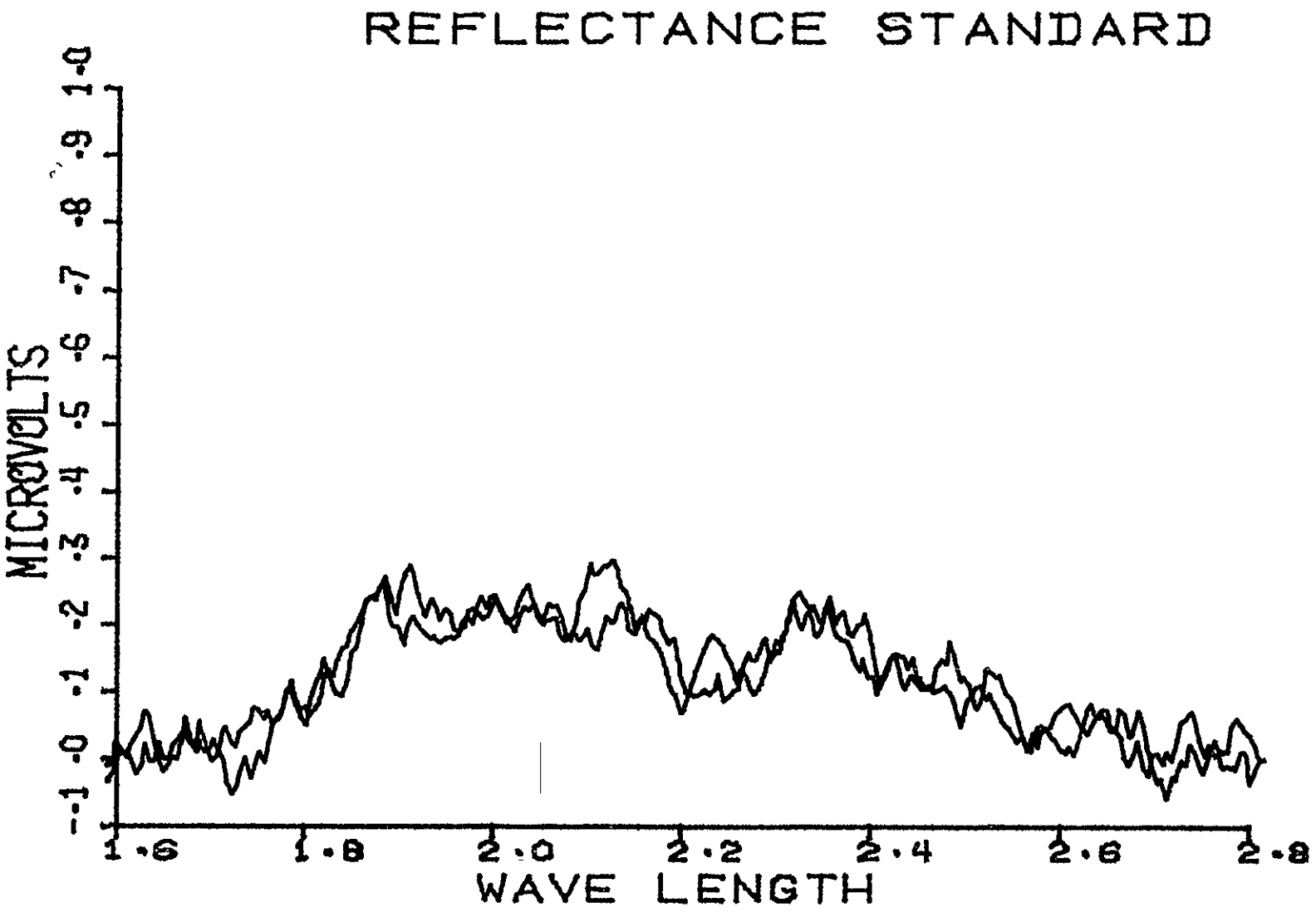
REFLECTANCE STANDARD
MICROVOLTS
-1 0 .1 .2 .3 .4 .5 .6 .7 .8 .9 1.0
1.6 1.8 2.0 2.2 2.4 2.6 2.8
WAVE LENGTH

FIG. 3

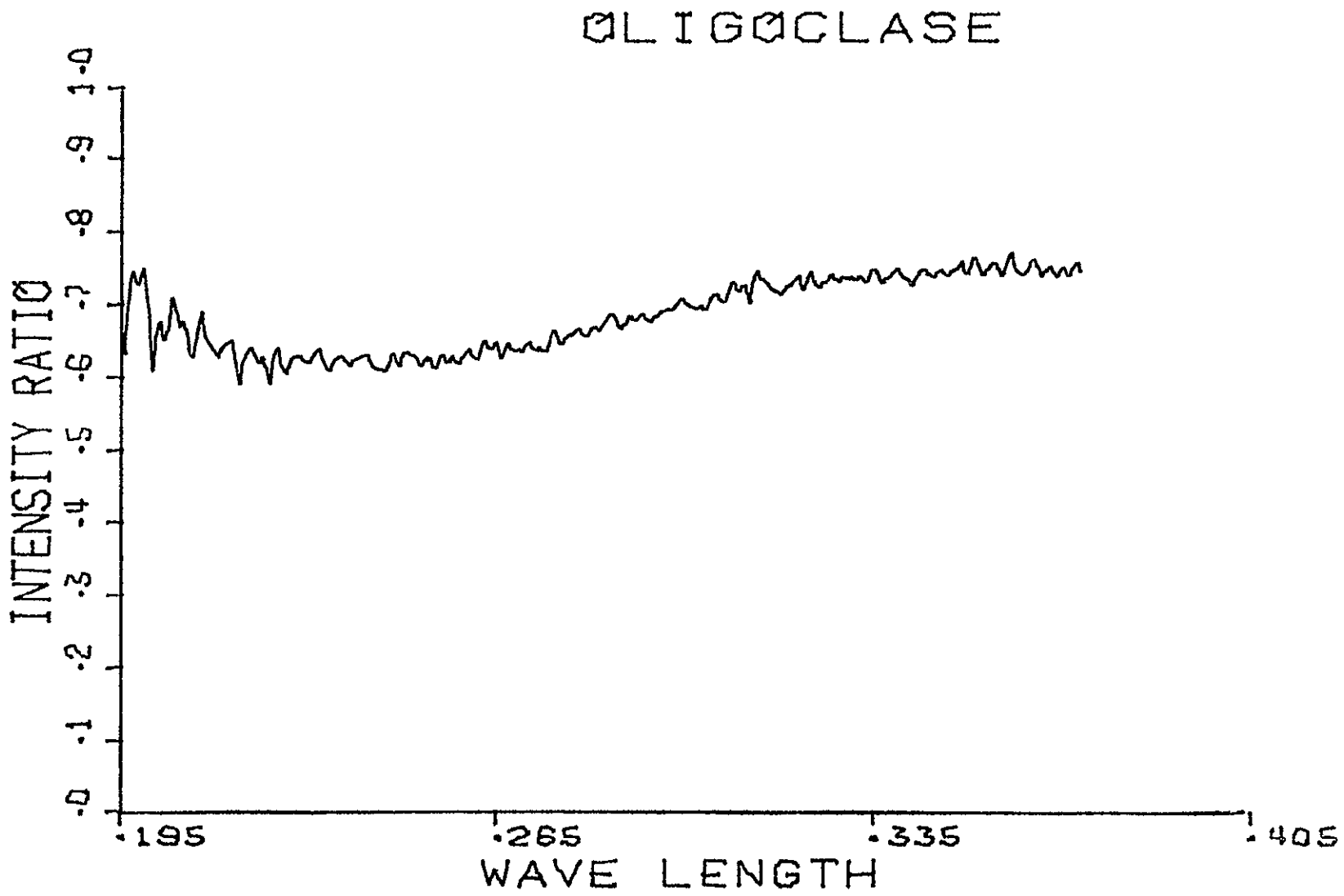
ØLIGØCLASE
INTENSITY RATIØ
.0
.1
.2
.3
.4
.5
.6
.7
.8
.9
1.0
.195
.265
.335
.405
WAVE LENGTH

FIG. 4a

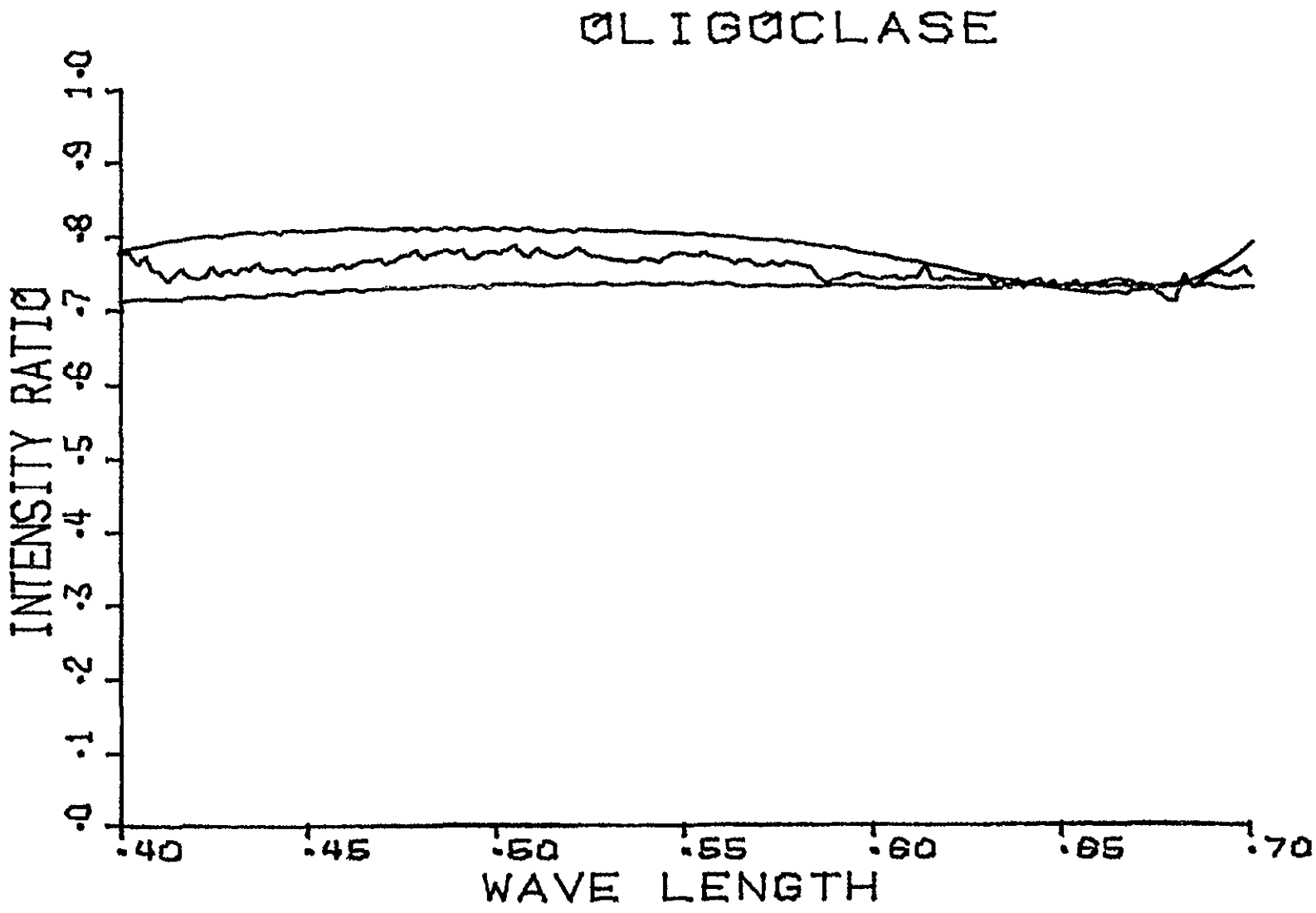
ØLIGØCLASE
INTENSITY RATIØ
·0
·1
·2
·3
·4
·5
·6
·7
·8
·9
1·0
·40
·45
·50
·55
·60
·65
·70
WAVE LENGTH

FIG. 4b

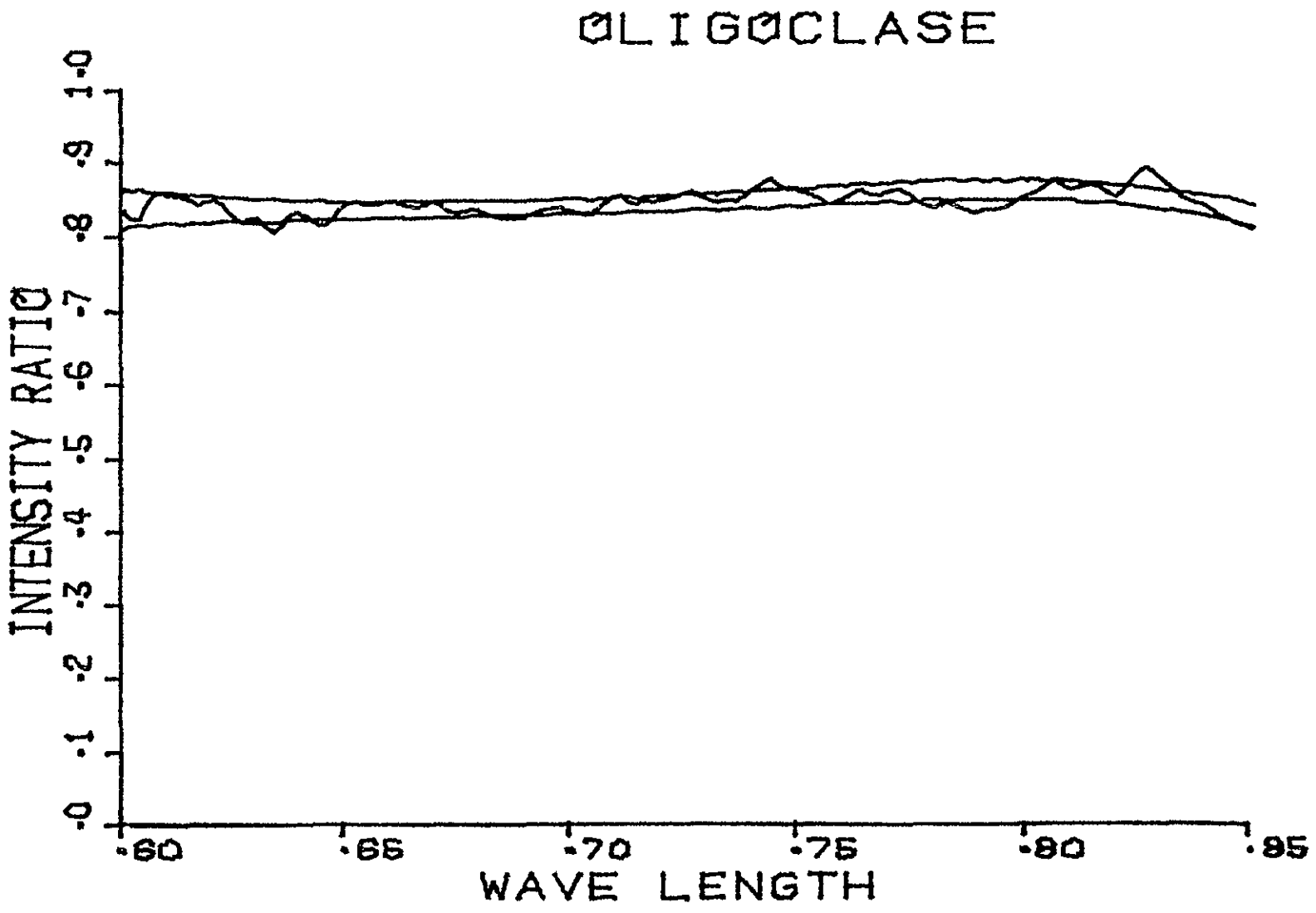
ØLIGØCLASE
INTENSITY RATIØ
·0
·1
·2
·3
·4
·5
·6
·7
·8
·9
1·0
·60
·65
·70
·75
·80
·85
WAVE LENGTH

FIG. 4c.

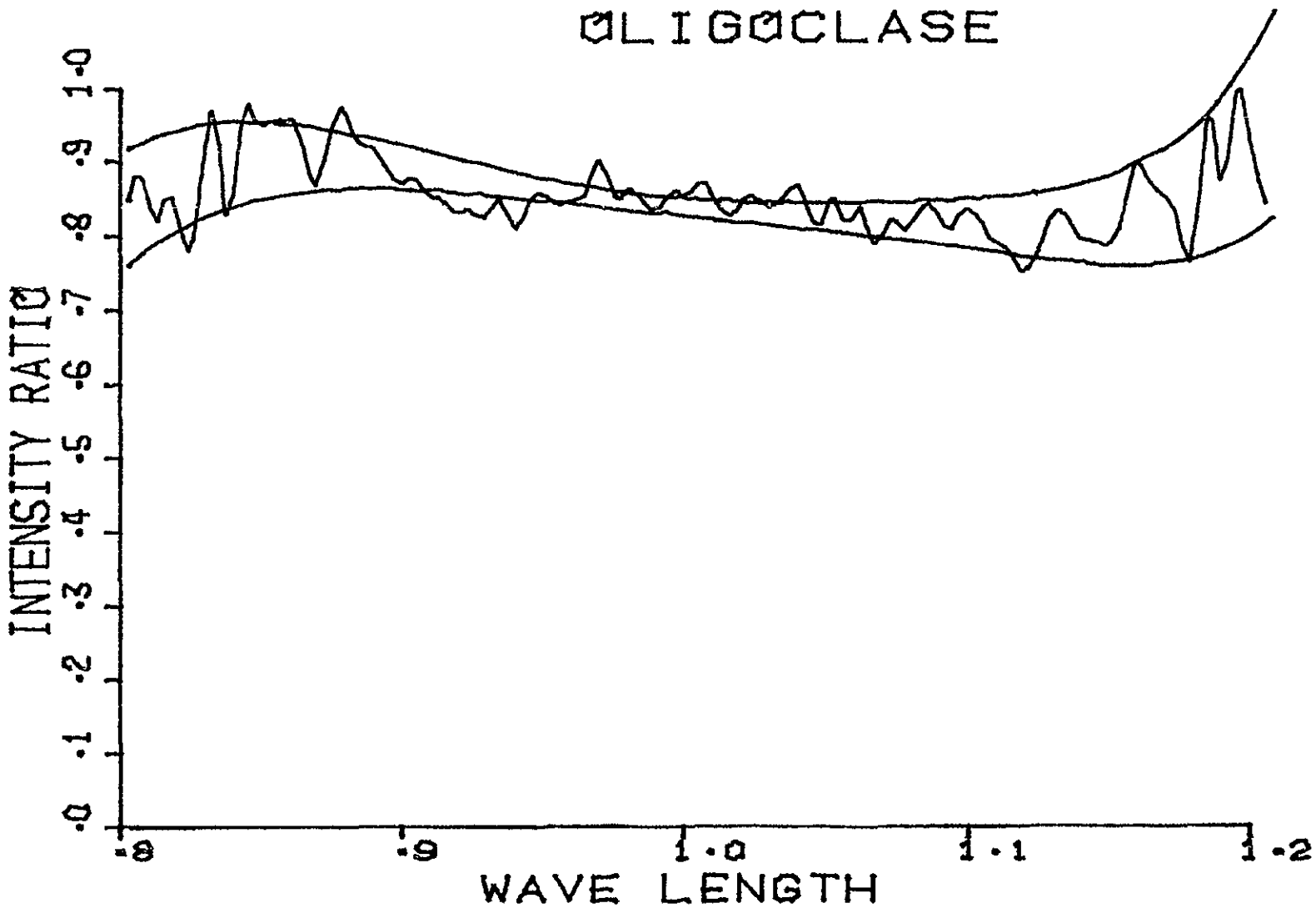
ØLIGØCLASE
INTENSITY RATIØ
0
.1
.2
.3
.4
.5
.6
.7
.8
.9
1.0
.8
.9
1.0
1.1
1.2
WAVE LENGTH

FIG. 4d

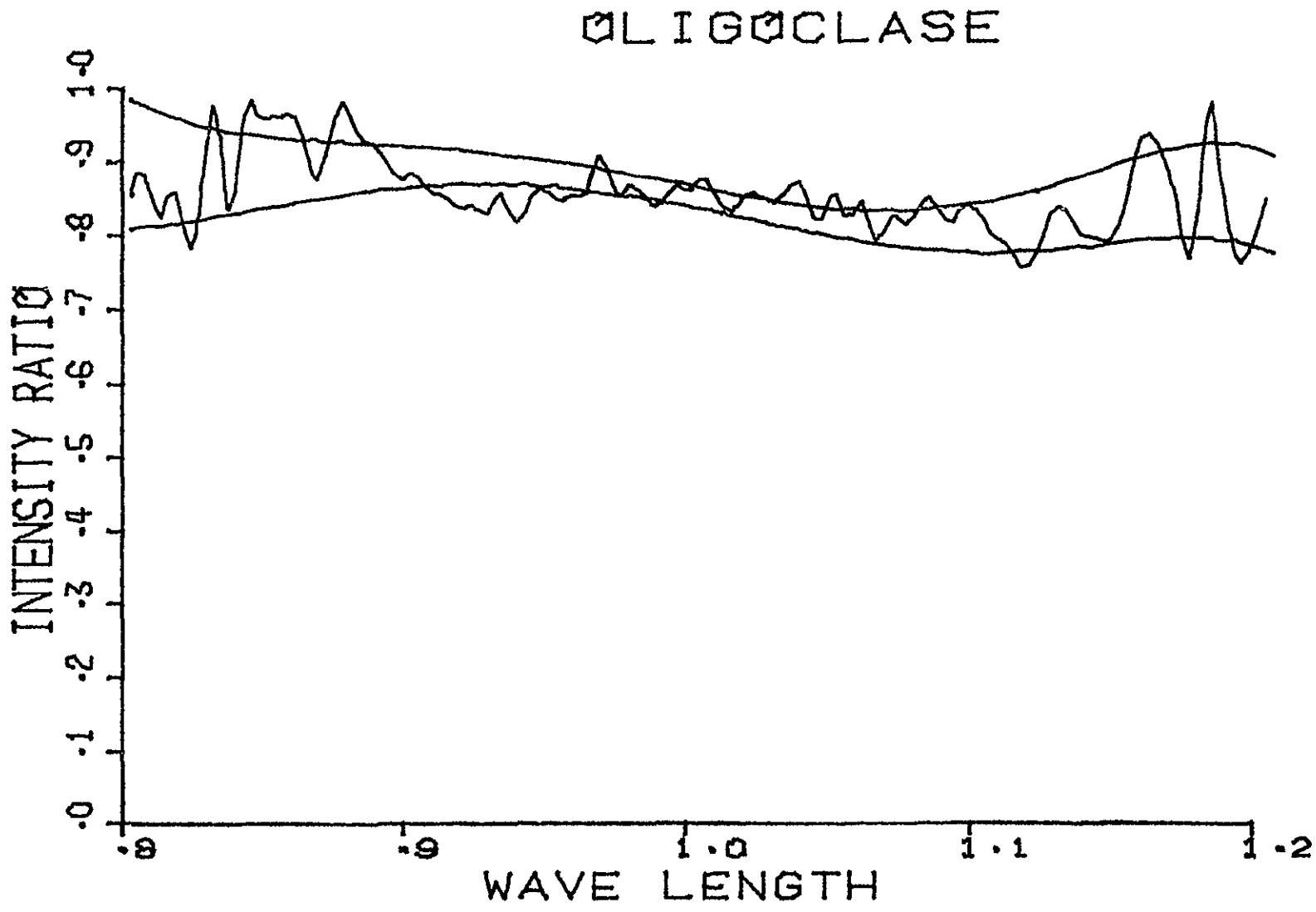
ØLIGØCLASE
INTENSITY RATIØ
0
.1
.2
.3
.4
.5
.6
.7
.8
.9
1.0
.8
.9
1.0
1.1
1.2
WAVE LENGTH

FIG. 4e

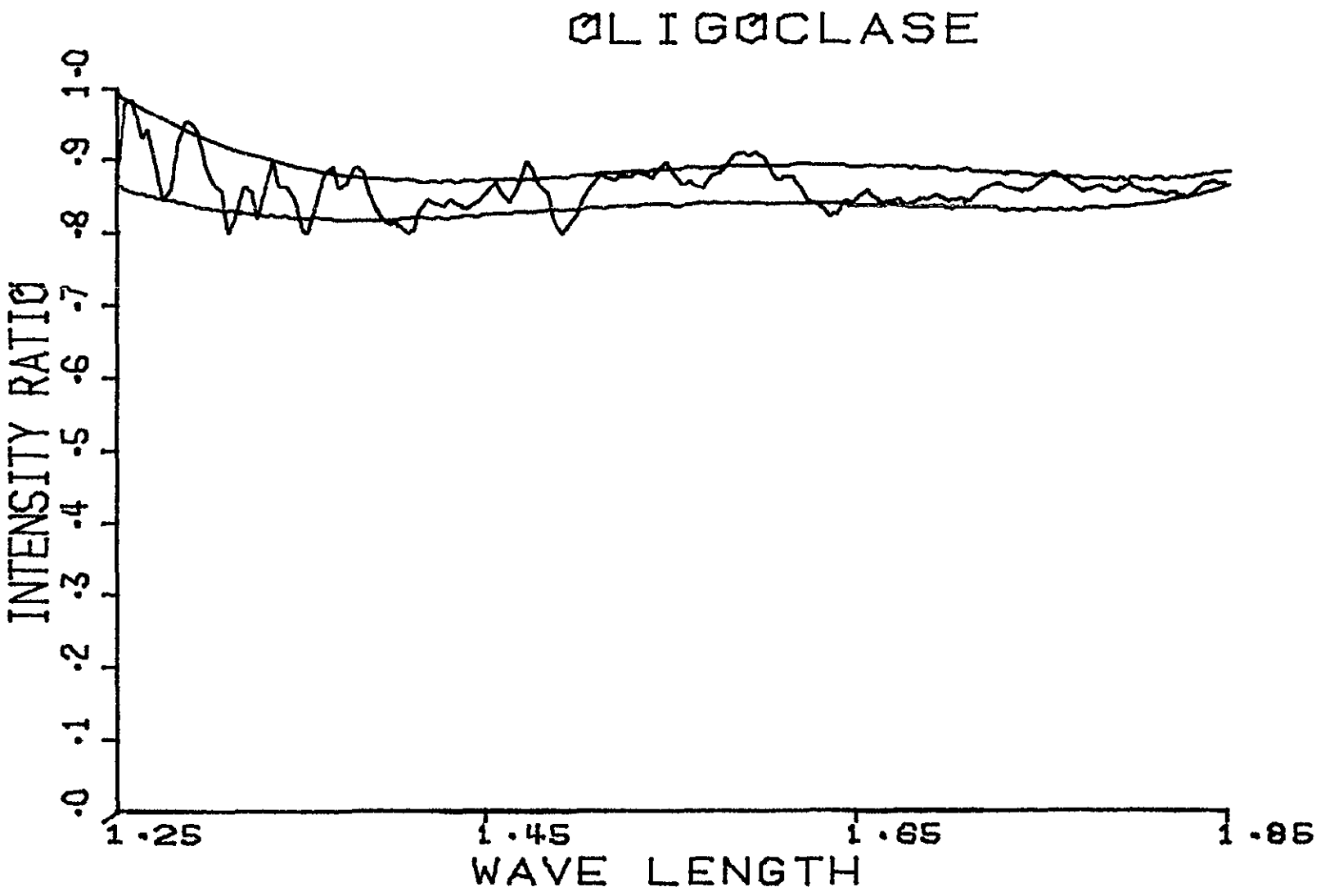
ØLIGØCLASE
INTENSITY RATIØ
.0
.1
.2
.3
.4
.5
.6
.7
.8
.9
1.0
1.25
1.45
1.65
1.85
WAVE LENGTH

FIG. 4f

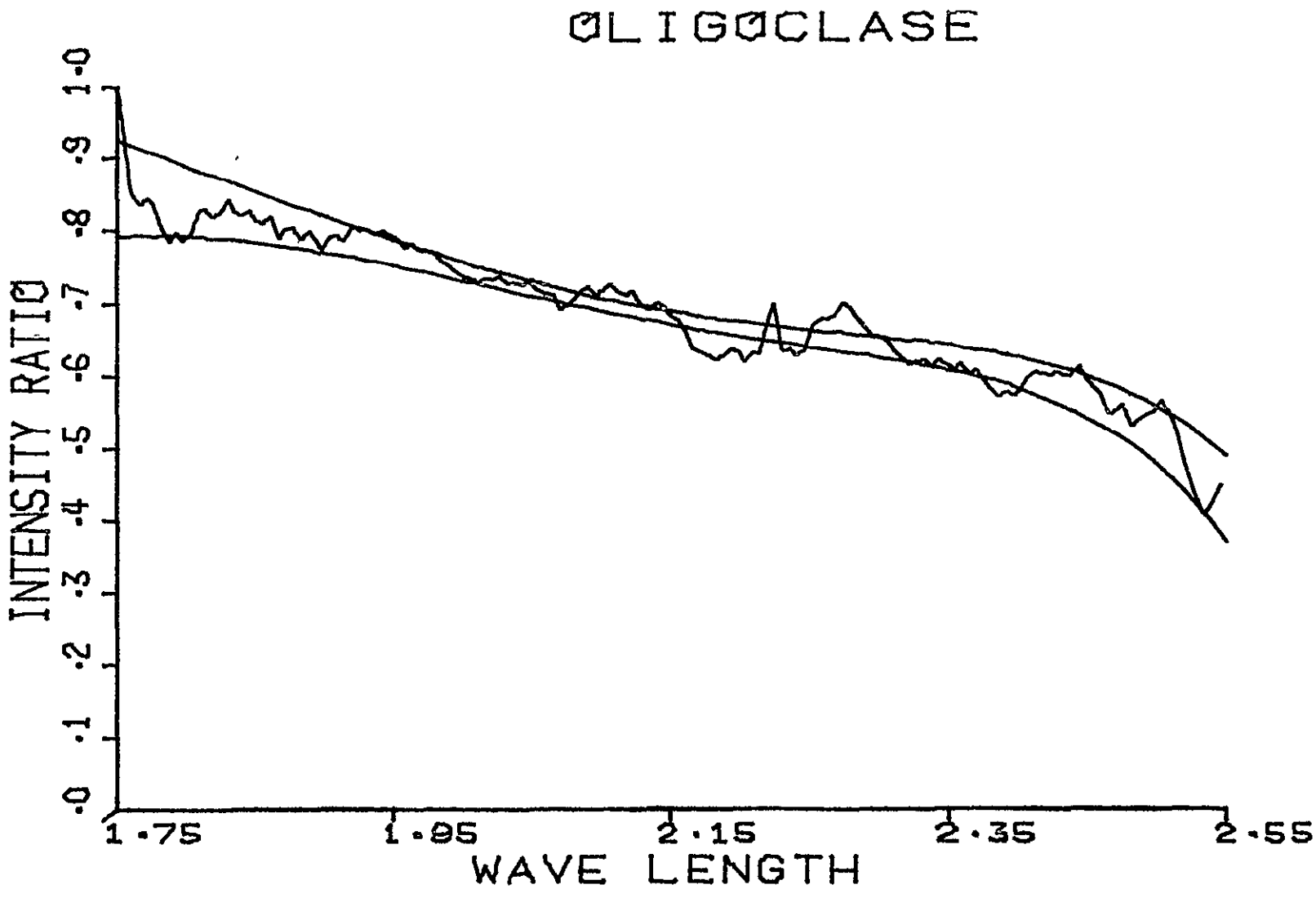
ØLIGØCLASE
INTENSITY RATIØ
.0
.1
.2
.3
.4
.5
.6
.7
.8
.9
1.0
1.75
1.95
2.15
2.35
2.55
WAVE LENGTH

FIG.4g

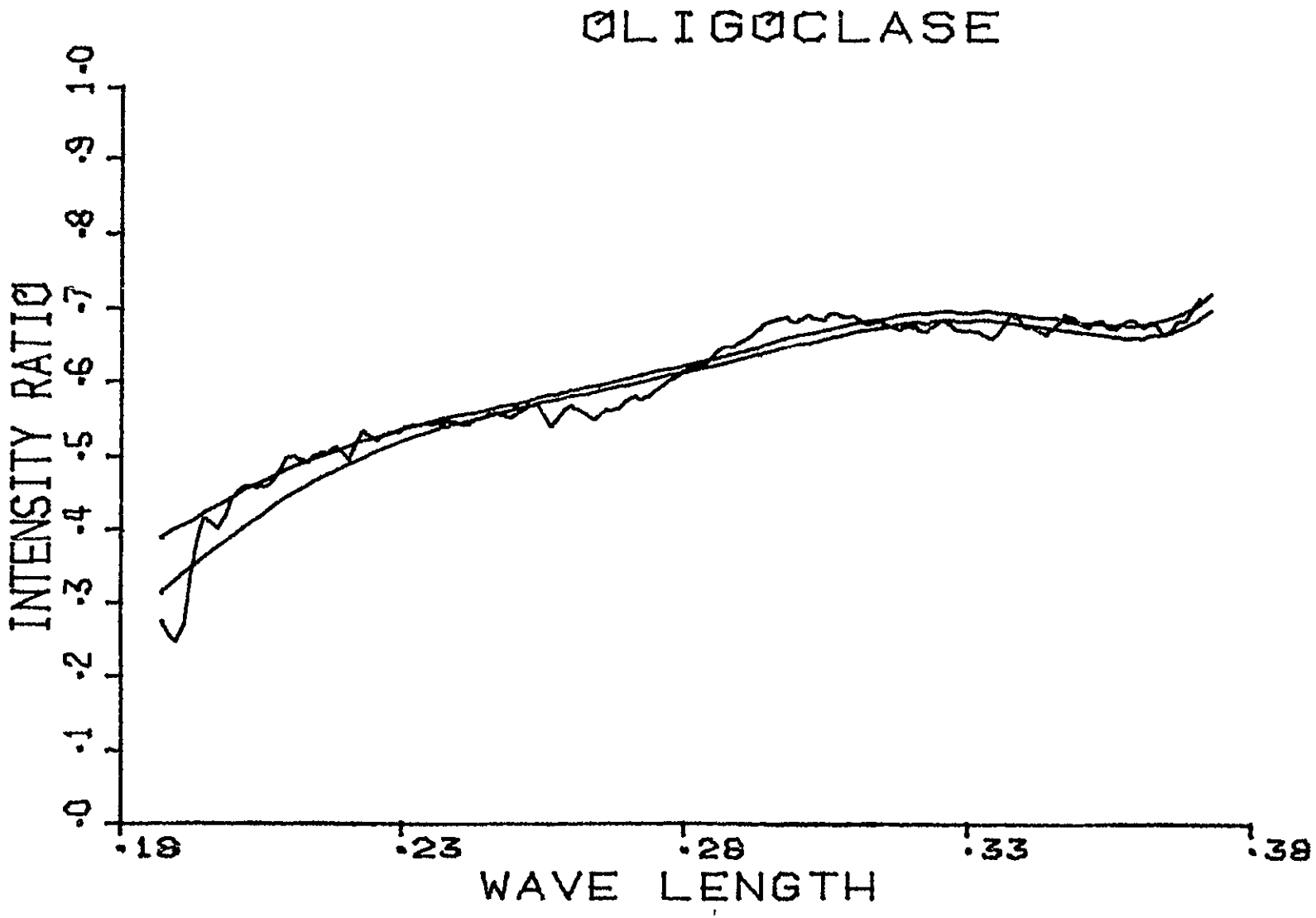
OLIGOCLASE
INTENSITY RATIO
0
.1
.2
.3
.4
.5
.6
.7
.8
.9
1.0
.18
.23
.28
.33
.38
WAVE LENGTH

FIG.5a

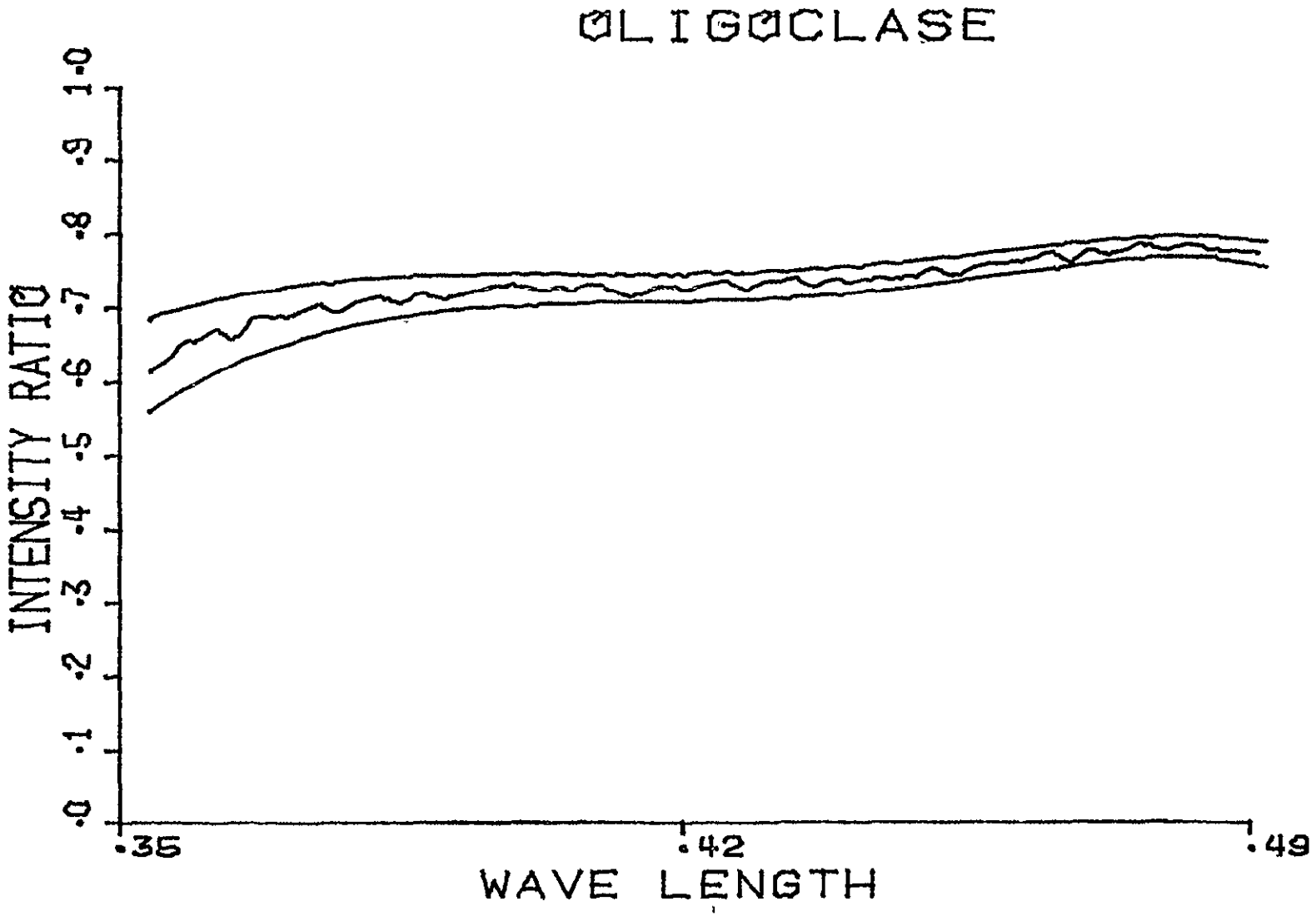
OLIGOCLASE
INTENSITY RATIO
0
.1
.2
.3
.4
.5
.6
.7
.8
.9
1.0
.35
.42
.49
WAVE LENGTH

FIG.5b

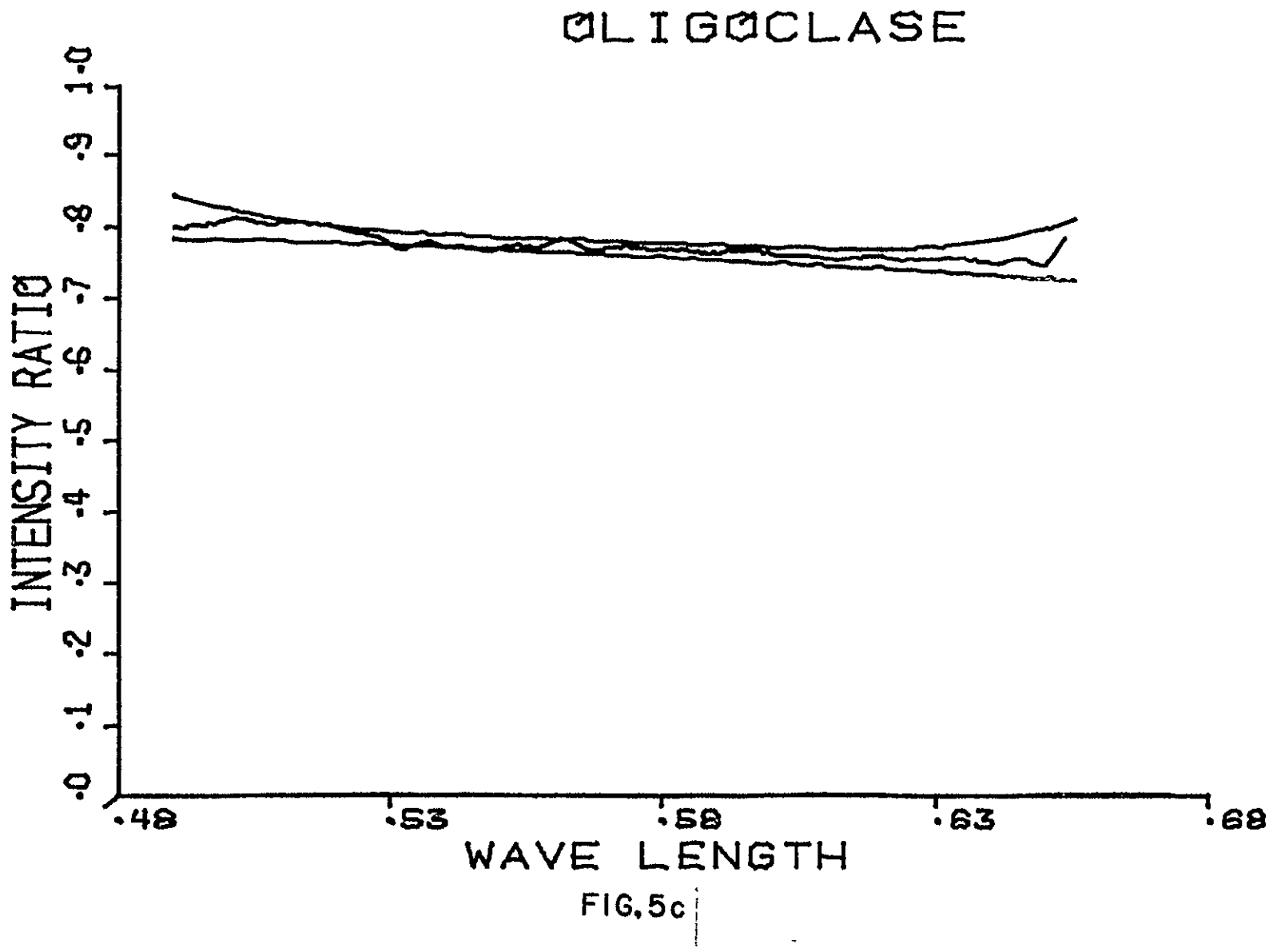
OLIGOCLASE
INTENSITY RATIO
.0
.1
.2
.3
.4
.5
.6
.7
.8
.9
1.0
.48
.53
.58
.63
.68
WAVE LENGTH

FIG. 5c

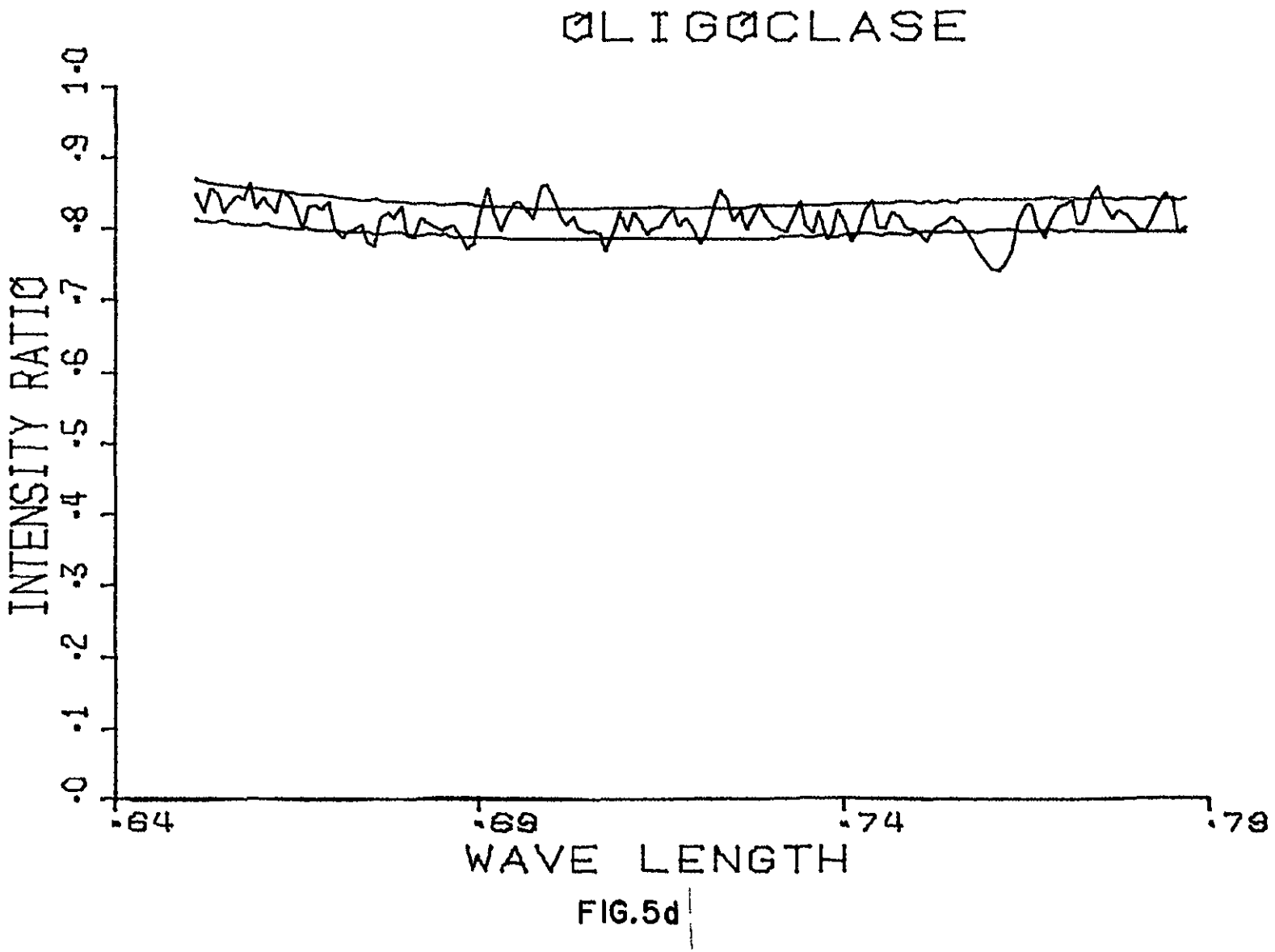
ØLIGØCLASE
INTENSITY RATIØ
.0
.1
.2
.3
.4
.5
.6
.7
.8
.9
1.0
.64
.69
.74
.79
WAVE LENGTH

FIG.5d

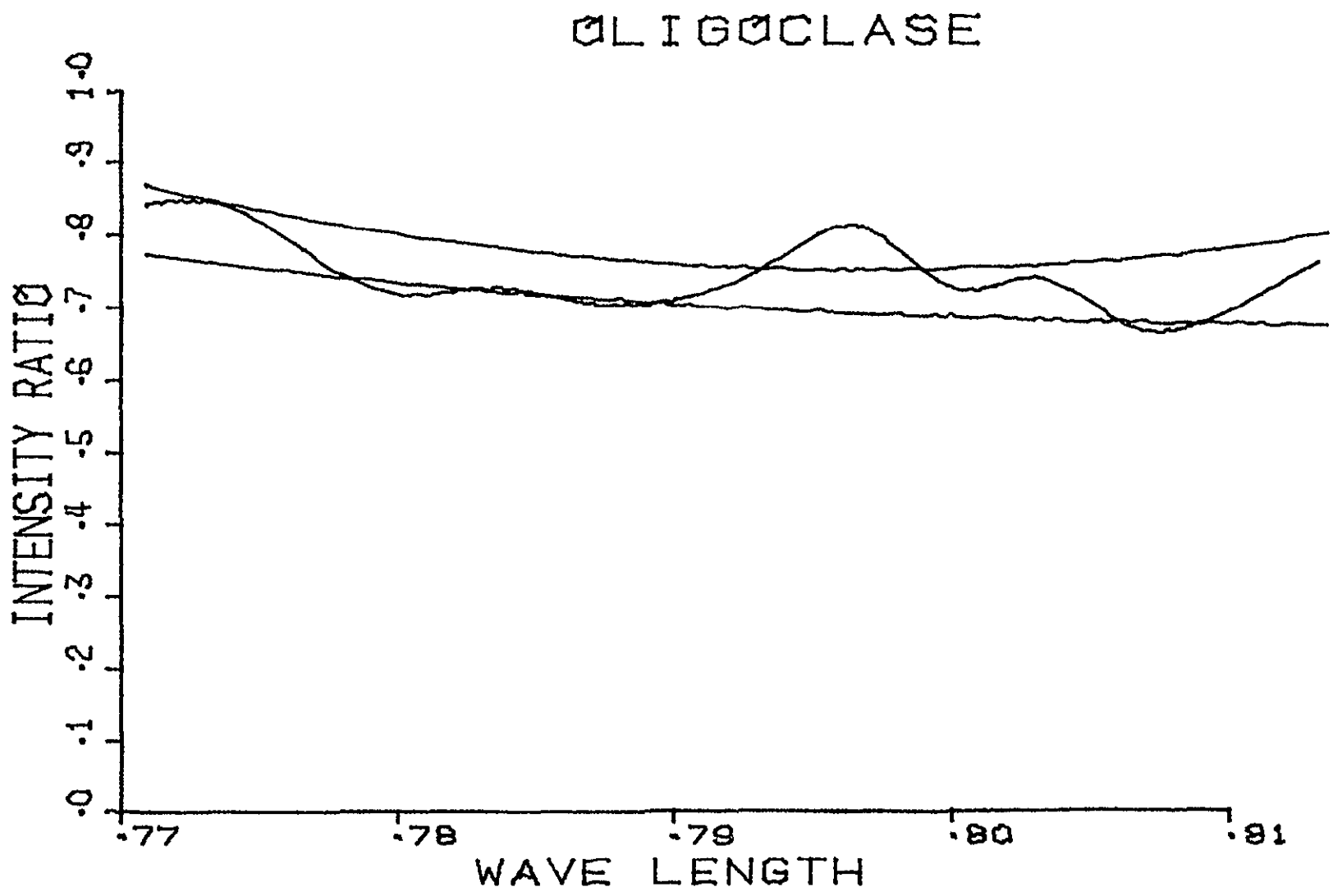
OLIGOCLASE
INTENSITY RATIO
.0
.1
.2
.3
.4
.5
.6
.7
.8
.9
1.0
.77
.78
.79
.80
.81
WAVE LENGTH

FIG.5e

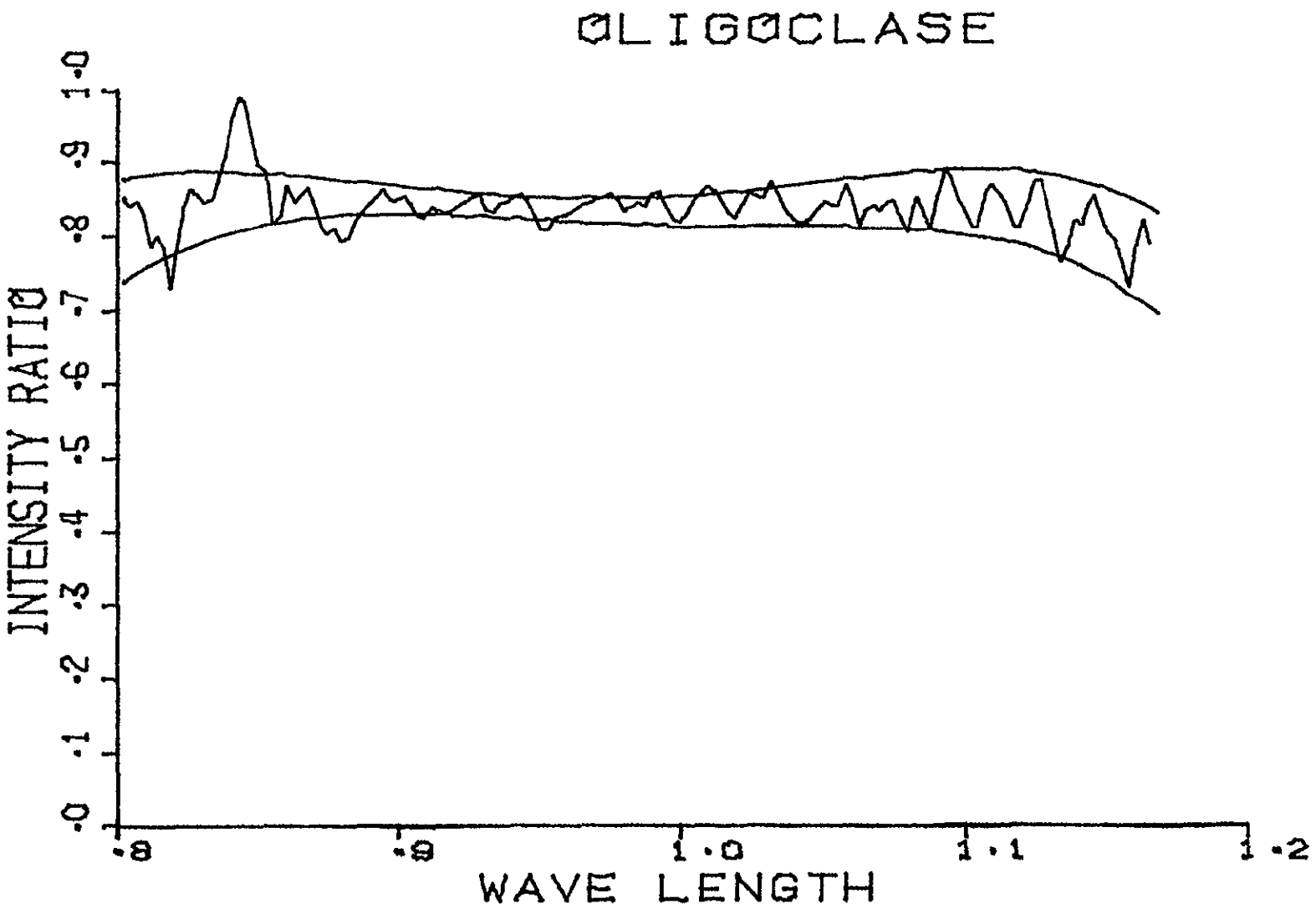
OLIGOCLASE
INTENSITY RATIO
0
.1
.2
.3
.4
.5
.6
.7
.8
.9
1.0
.8
.9
1.0
1.1
1.2
WAVE LENGTH

FIG. 5f

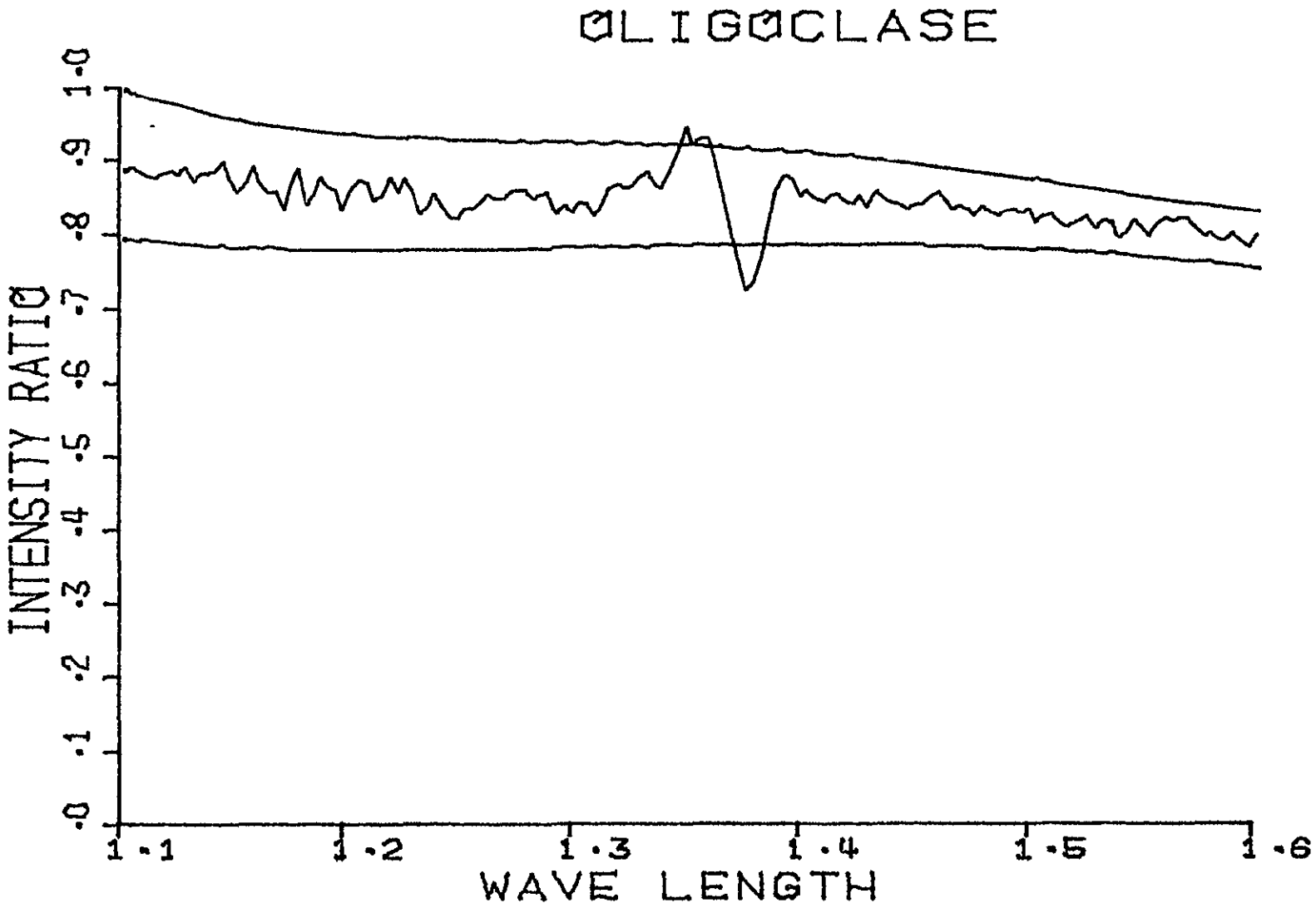
OLIGOCLASE
INTENSITY RATIO
.0
.1
.2
.3
.4
.5
.6
.7
.8
.9
1.0
1.1
1.2
1.3
1.4
1.5
1.6
WAVE LENGTH

FIG.5g

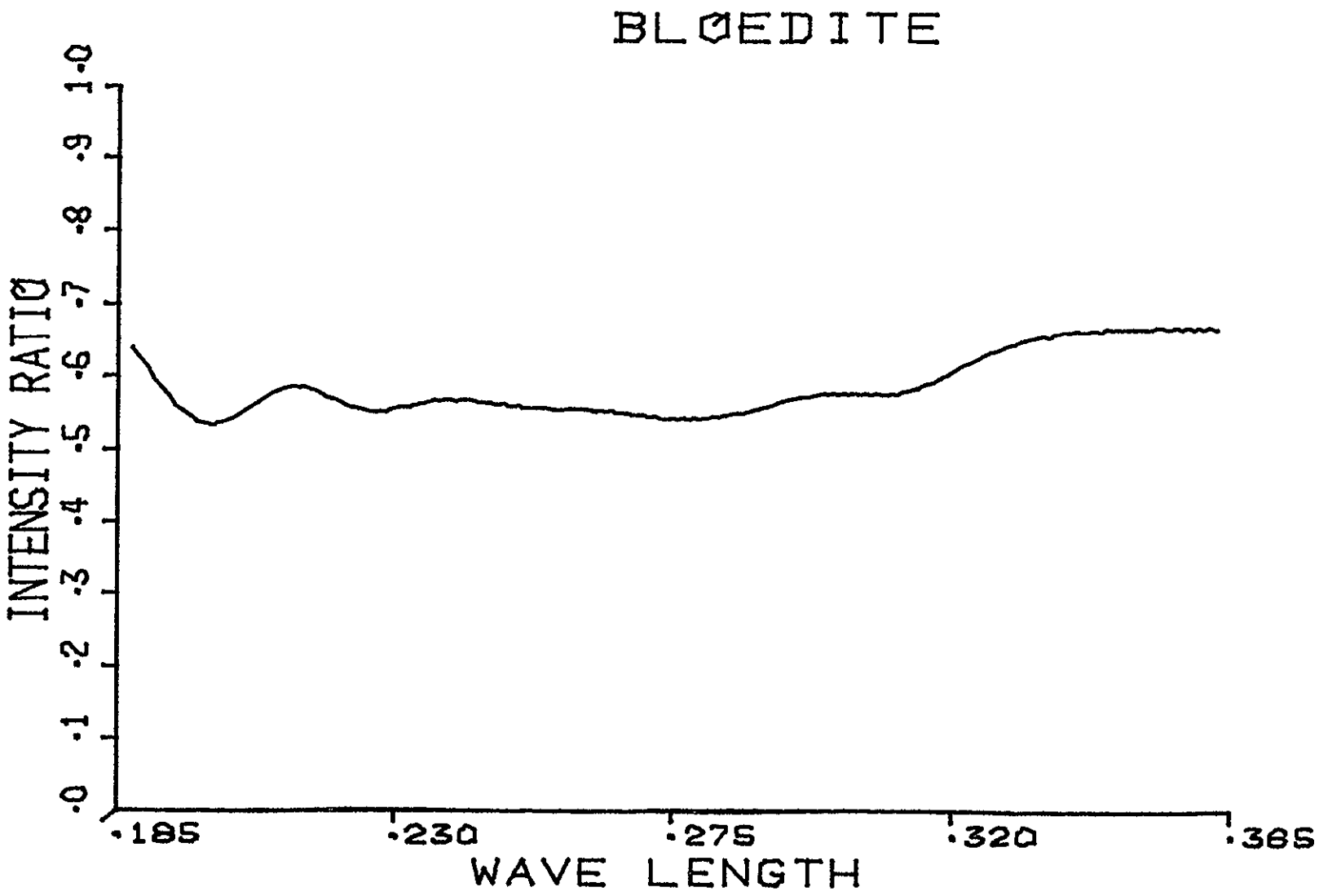
BLØEDITE
INTENSITY RATIØ
.0
.1
.2
.3
.4
.5
.6
.7
.8
.9
1.0
.185
.230
.275
.320
.365
WAVE LENGTH

FIG.6a

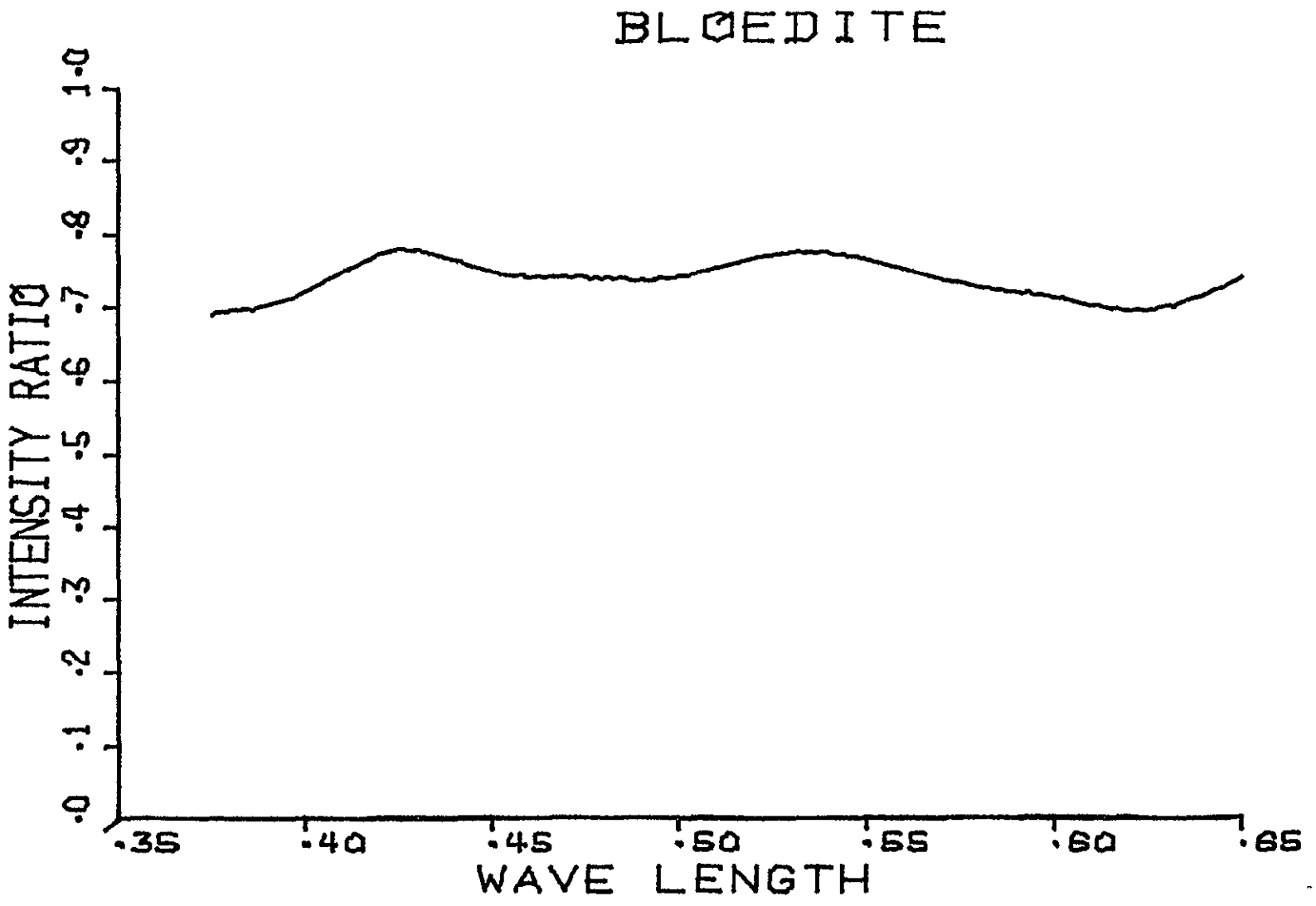
BLOEDITE
INTENSITY RATIO
0
.1
.2
.3
.4
.5
.6
.7
.8
.9
1.0
.35
.40
.45
.50
.55
.60
.65
WAVE LENGTH

FIG.6b

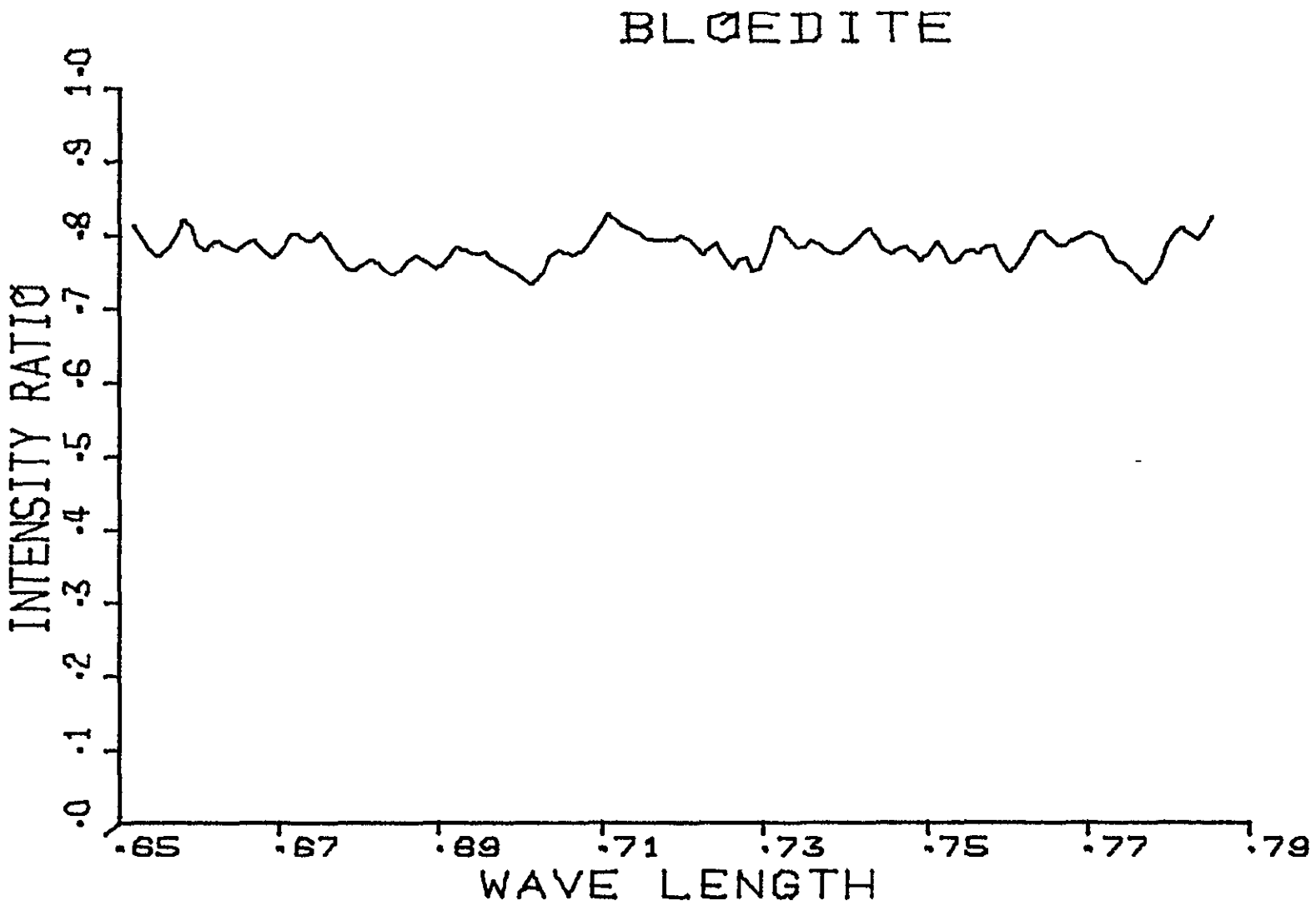
BLØEDITE
INTENSITY RATIØ
.0
.1
.2
.3
.4
.5
.6
.7
.8
.9
1.0
.65
.67
.69
.71
.73
.75
.77
.79
WAVE LENGTH

FIG.6c

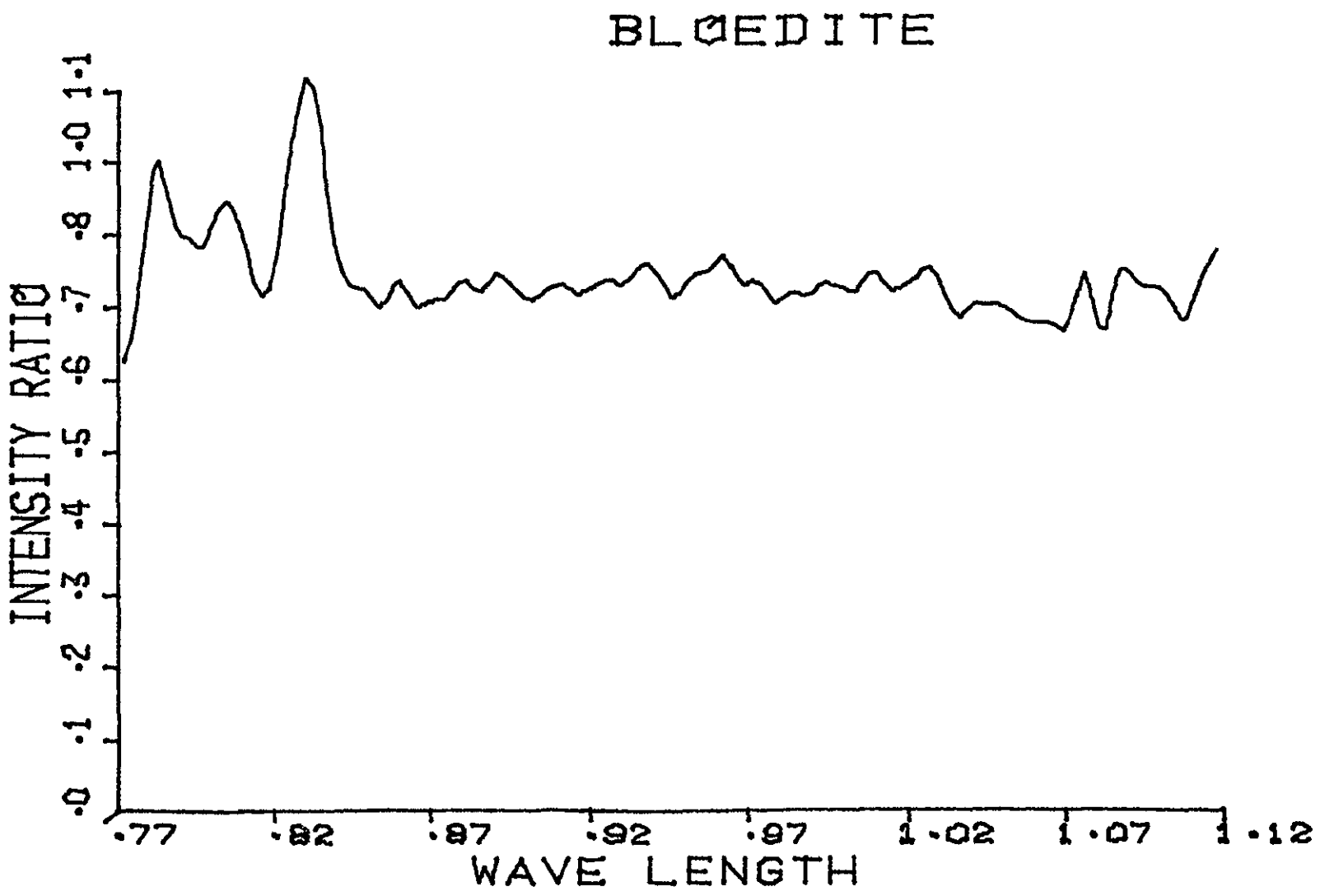
BLOEDITE
INTENSITY RATIO
0
.1
.2
.3
.4
.5
.6
.7
.8
1.0
1.1
.77
.82
.87
.92
.97
1.02
1.07
1.12
WAVE LENGTH

FIG.6d

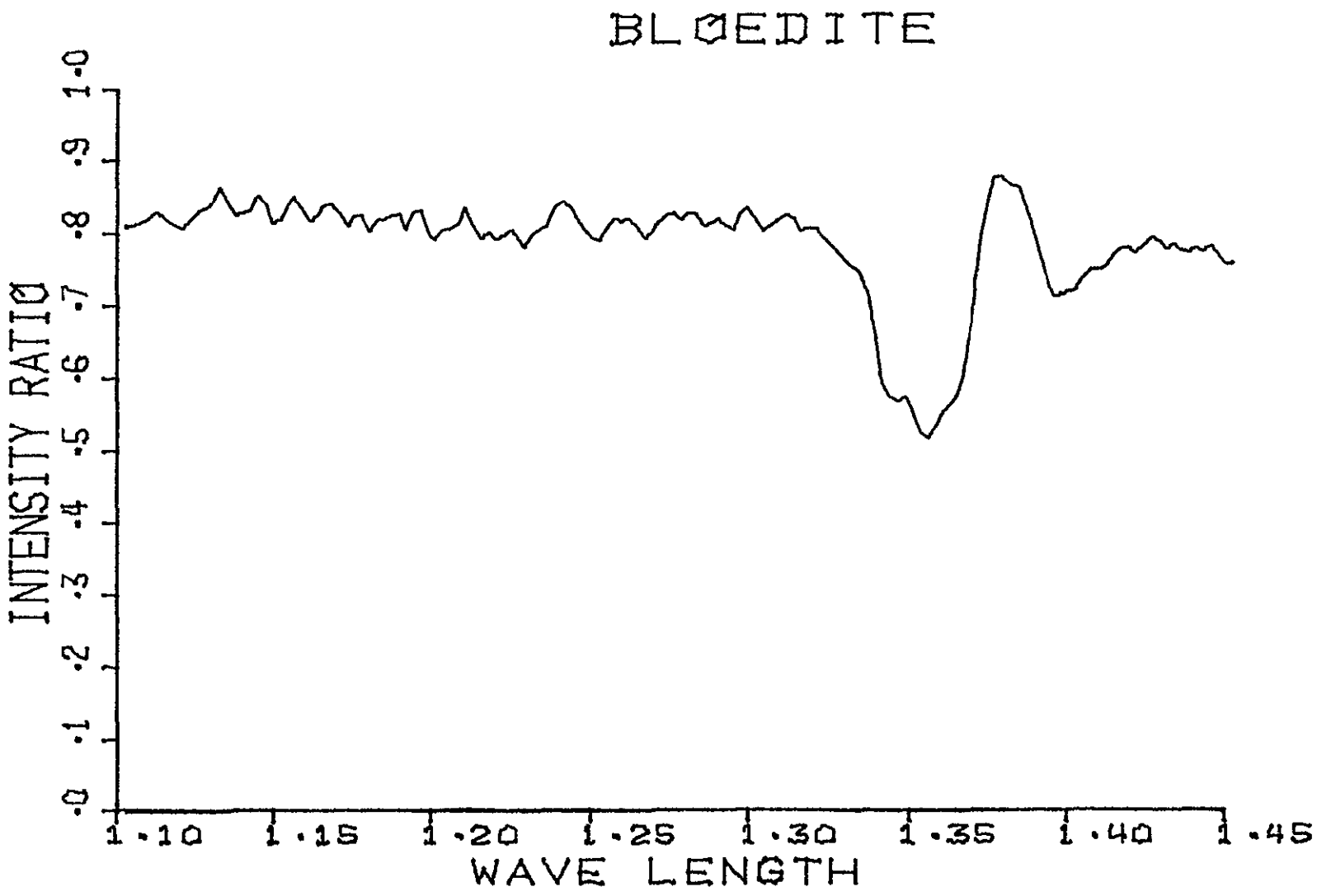
BLØEDITE
INTENSITY RATIØ
.0
.1
.2
.3
.4
.5
.6
.7
.8
.9
1.0
1.10
1.15
1.20
1.25
1.30
1.35
1.40
1.45
WAVE LENGTH

FIG. 6e

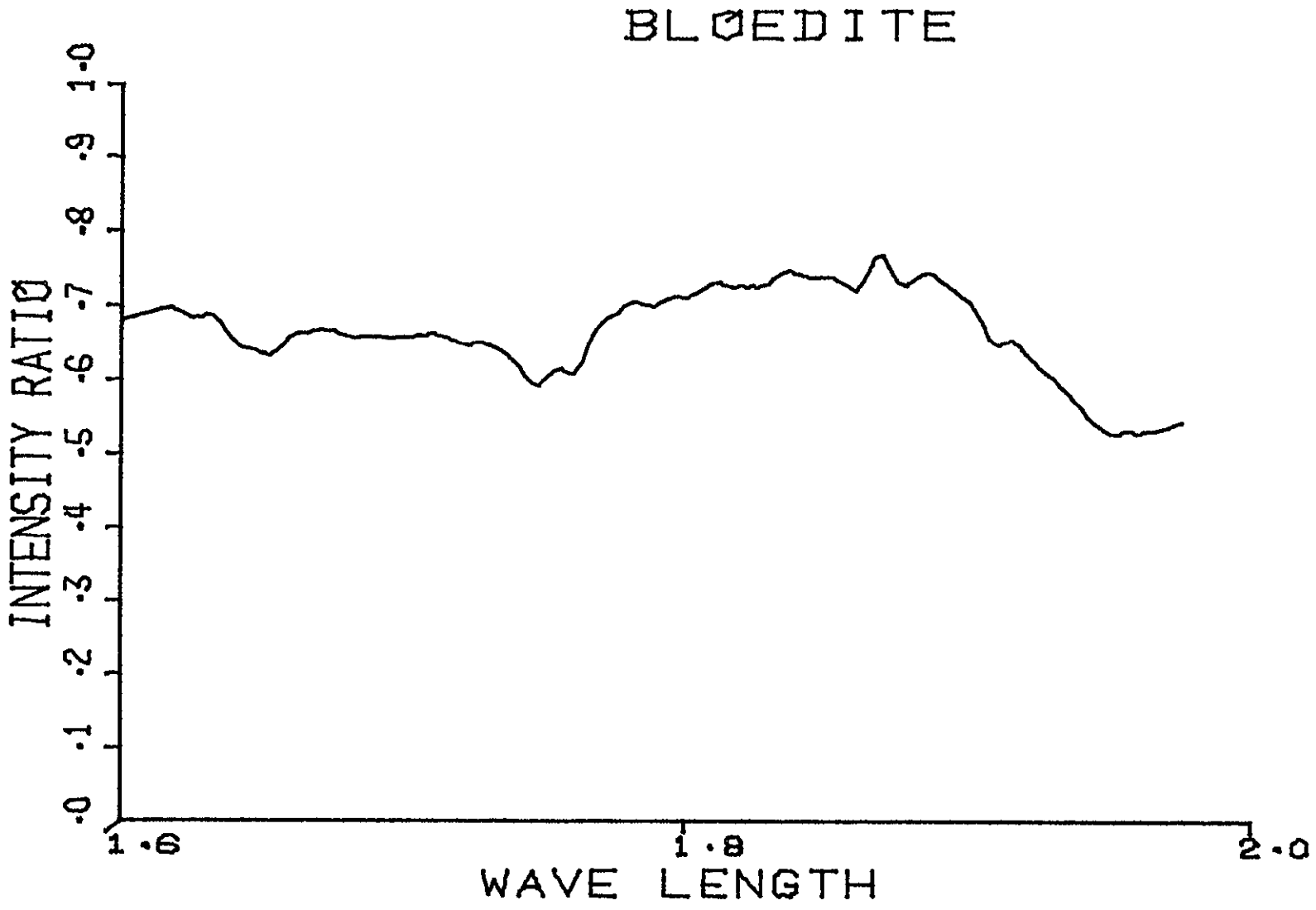
BLOEDITE
INTENSITY RATIO
0·0
·1
·2
·3
·4
·5
·6
·7
·8
·9
1·0
1·6
1·8
2·0
WAVE LENGTH

FIG.6f

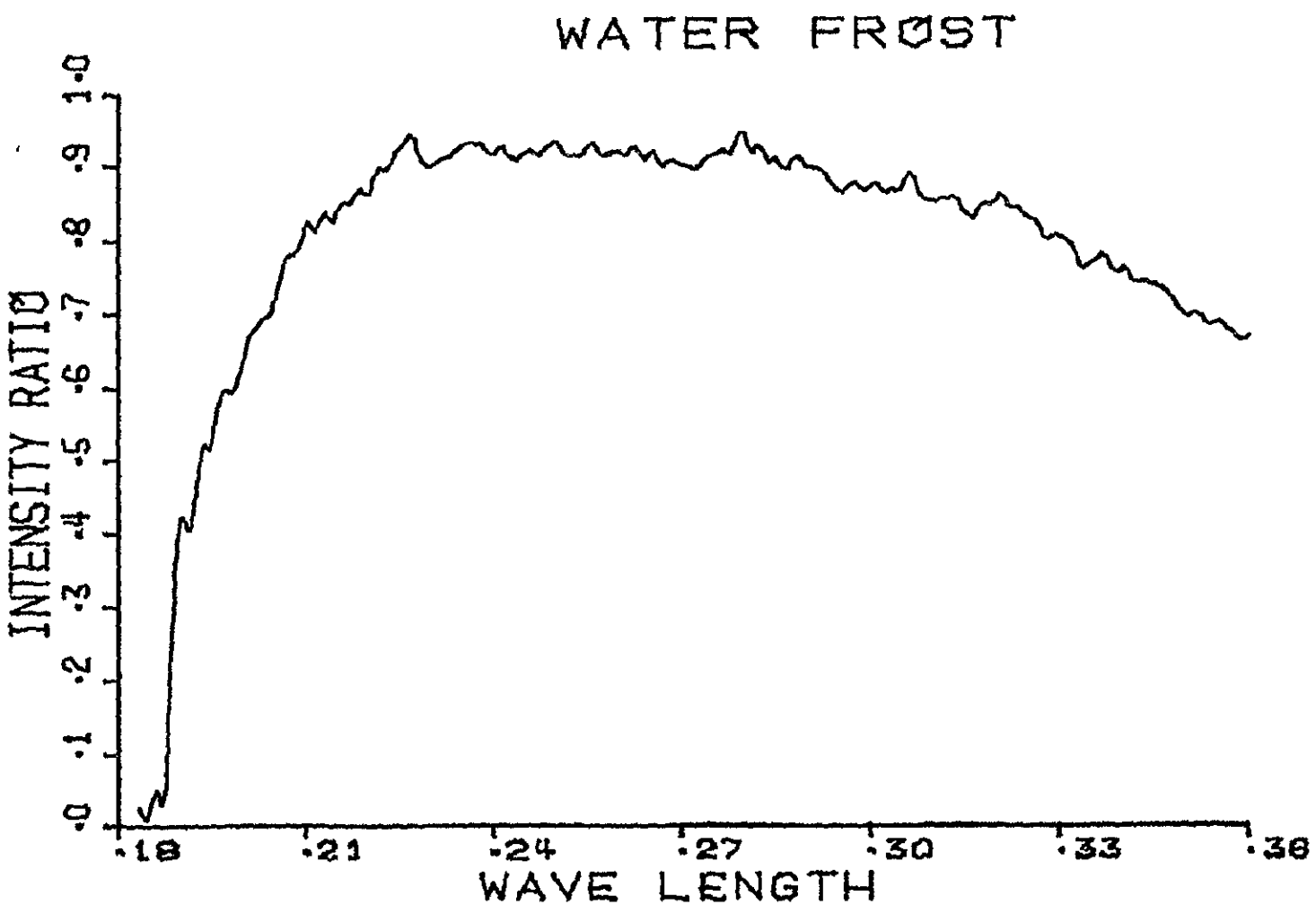
WATER FROST
INTENSITY RATIO
.0
.1
.2
.3
.4
.5
.6
.7
.8
.9
1.0
.18
.21
.24
.27
.30
.33
.36
WAVE LENGTH

FIG. 7a

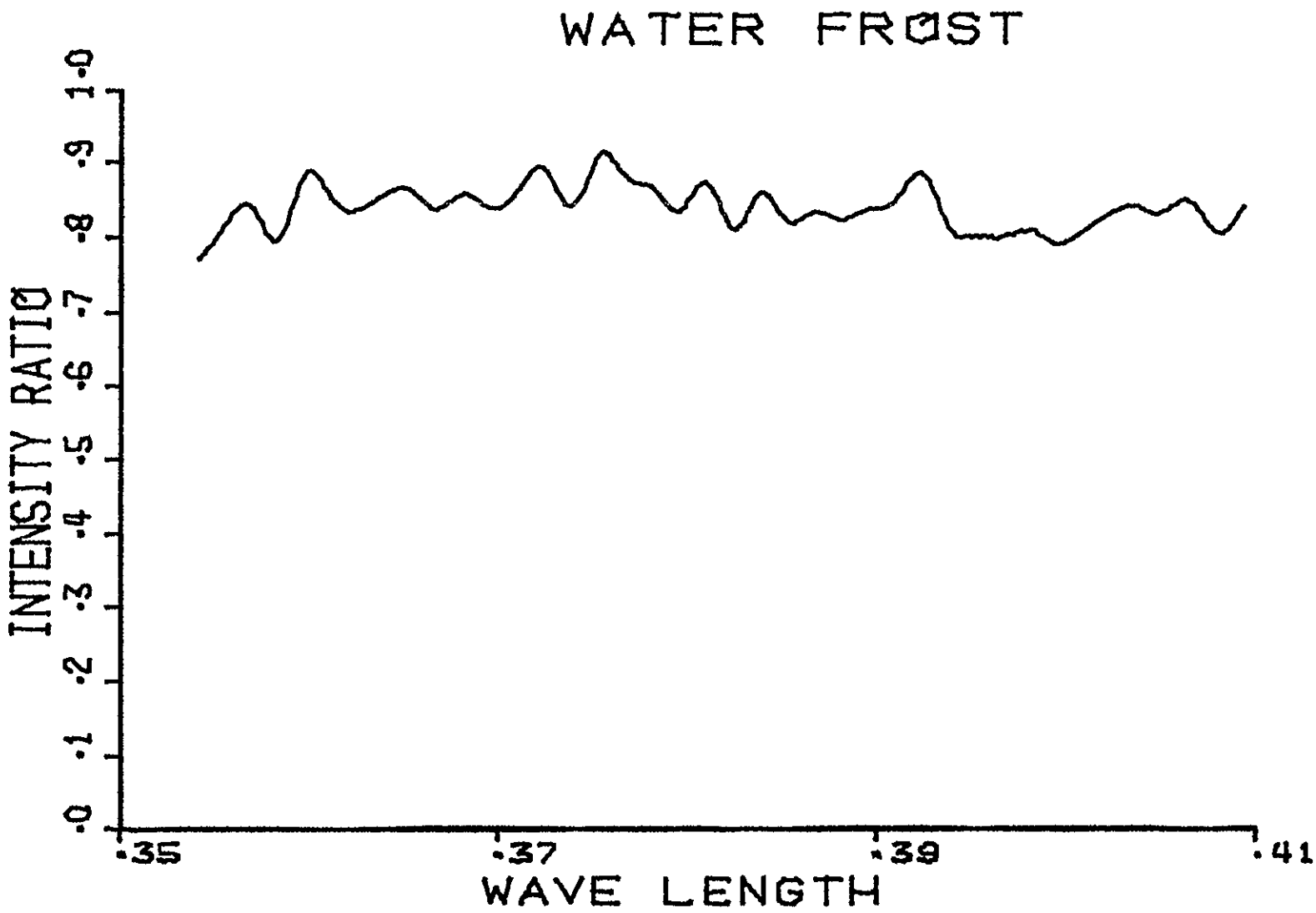
WATER FROST
INTENSITY RATIO
0
.1
.2
.3
.4
.5
.6
.7
.8
.9
1.0
.35
.37
.39
.41
WAVE LENGTH

FIG.7b

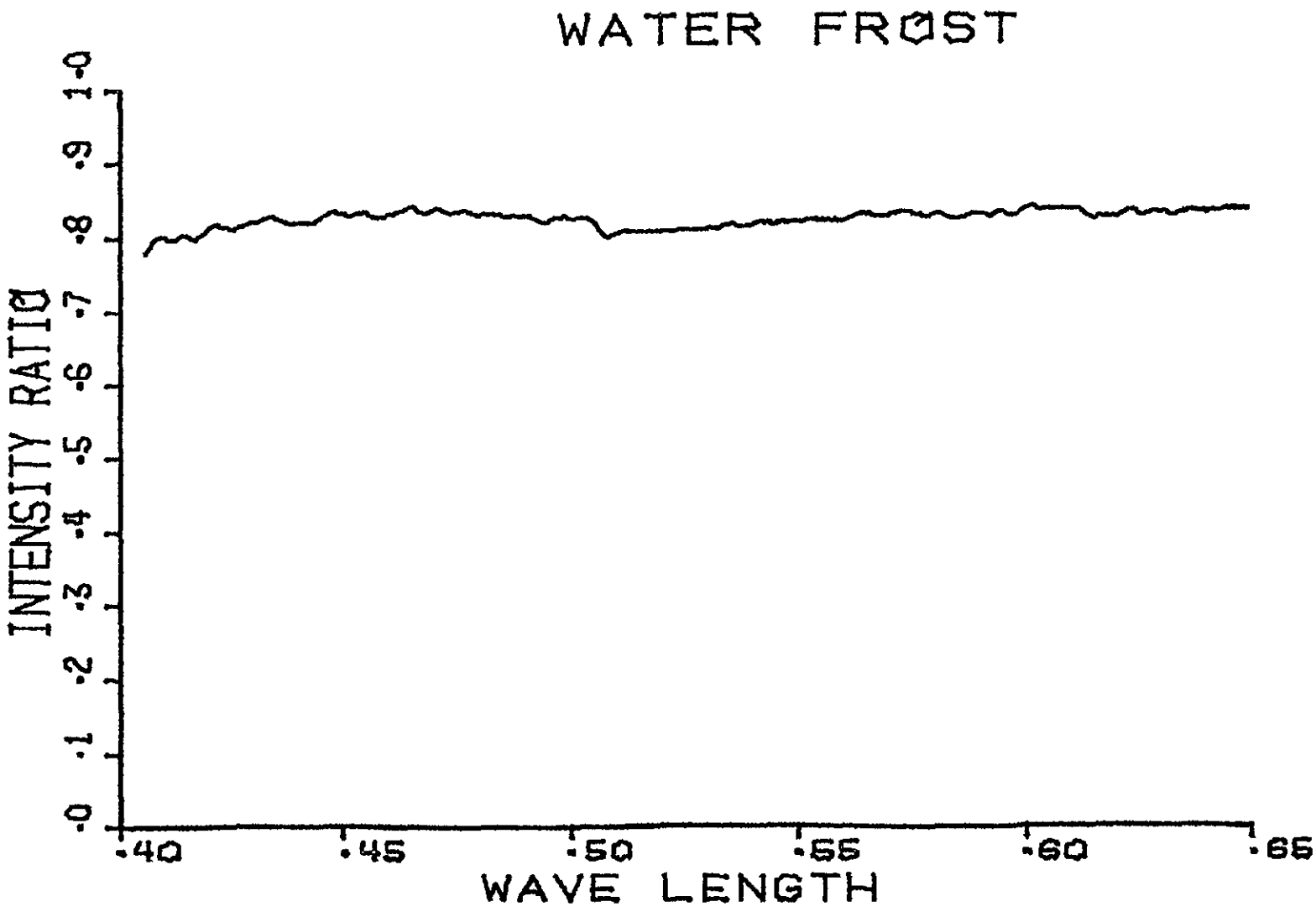
WATER FROST
INTENSITY RATIO
0
.1
.2
.3
.4
.5
.6
.7
.8
.9
1.0
.40
.45
.50
.55
.60
.65
WAVE LENGTH

FIG.7c

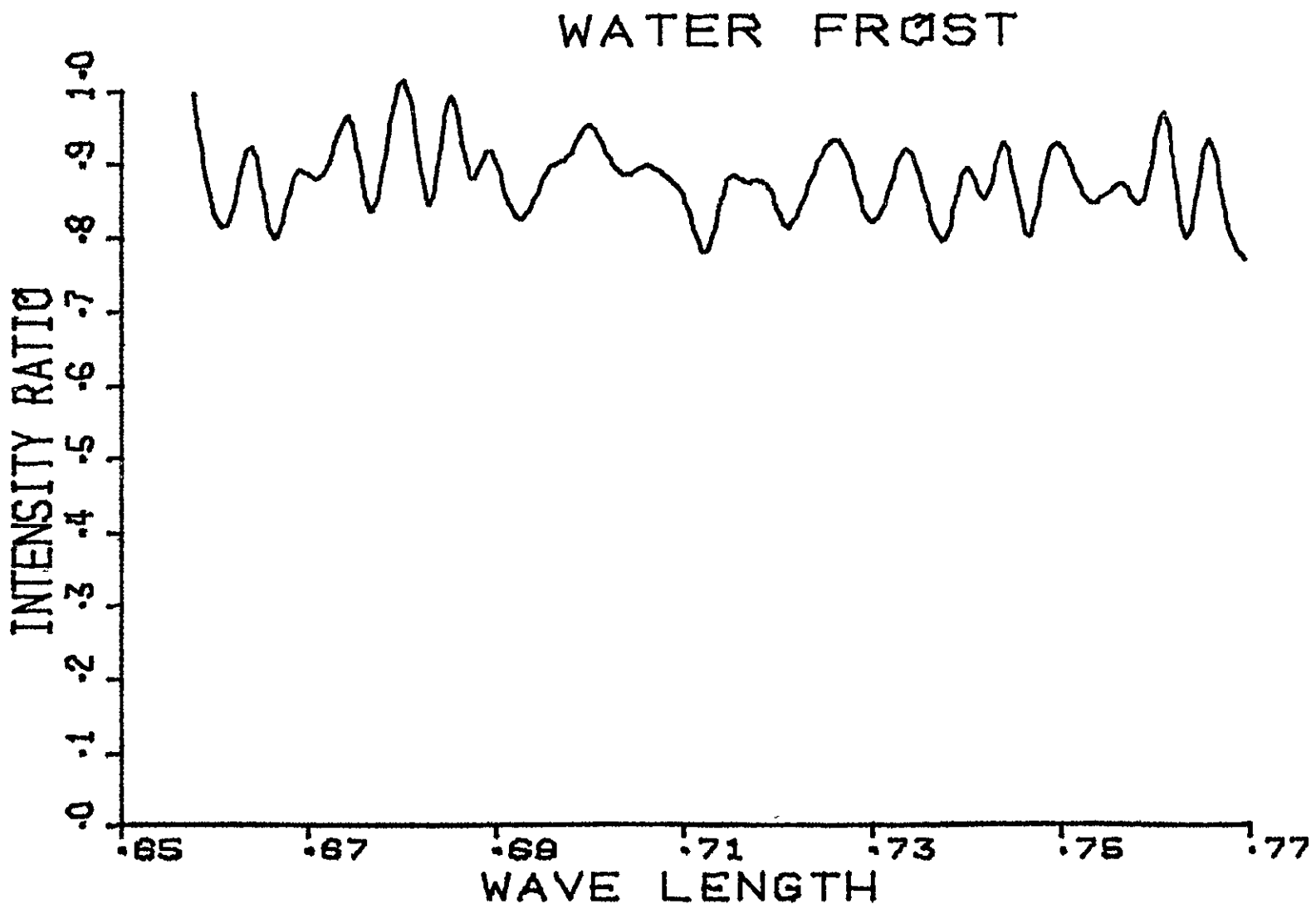
WATER FROST
INTENSITY RATIO
.0
.1
.2
.3
.4
.5
.6
.7
.8
.9
1.0
.65
.67
.69
.71
.73
.75
.77
WAVE LENGTH

FIG. 7d

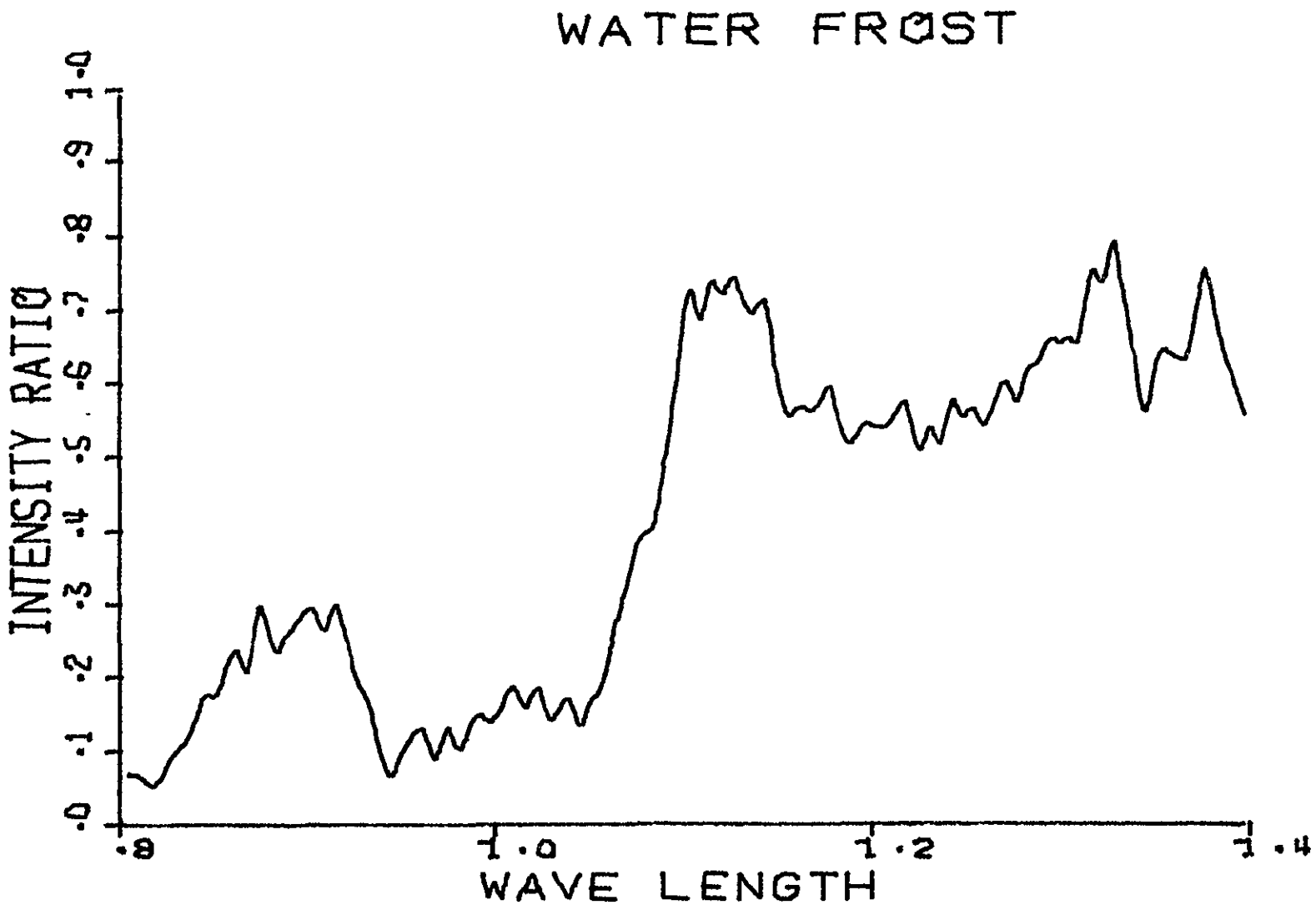
WATER FROST
INTENSITY RATIO
.0
.1
.2
.3
.4
.5
.6
.7
.8
.9
1.0
.8
1.0
1.2
1.4
WAVE LENGTH

FIG. 7e

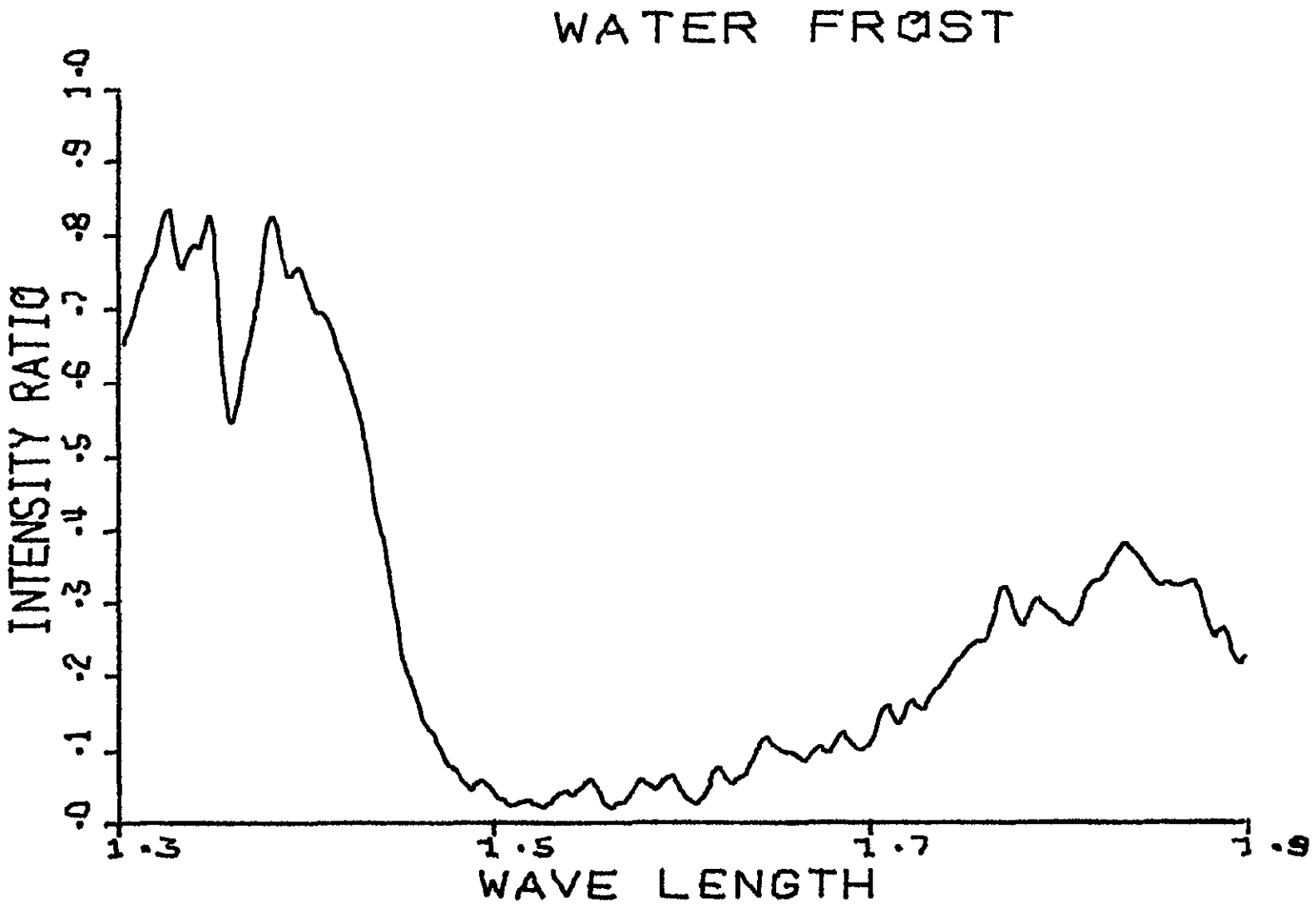
WATER FROST
INTENSITY RATIO
0
.1
.2
.3
.4
.5
.6
.7
.8
.9
1.0
1.3
1.5
1.7
1.9
WAVE LENGTH

FIG.7f

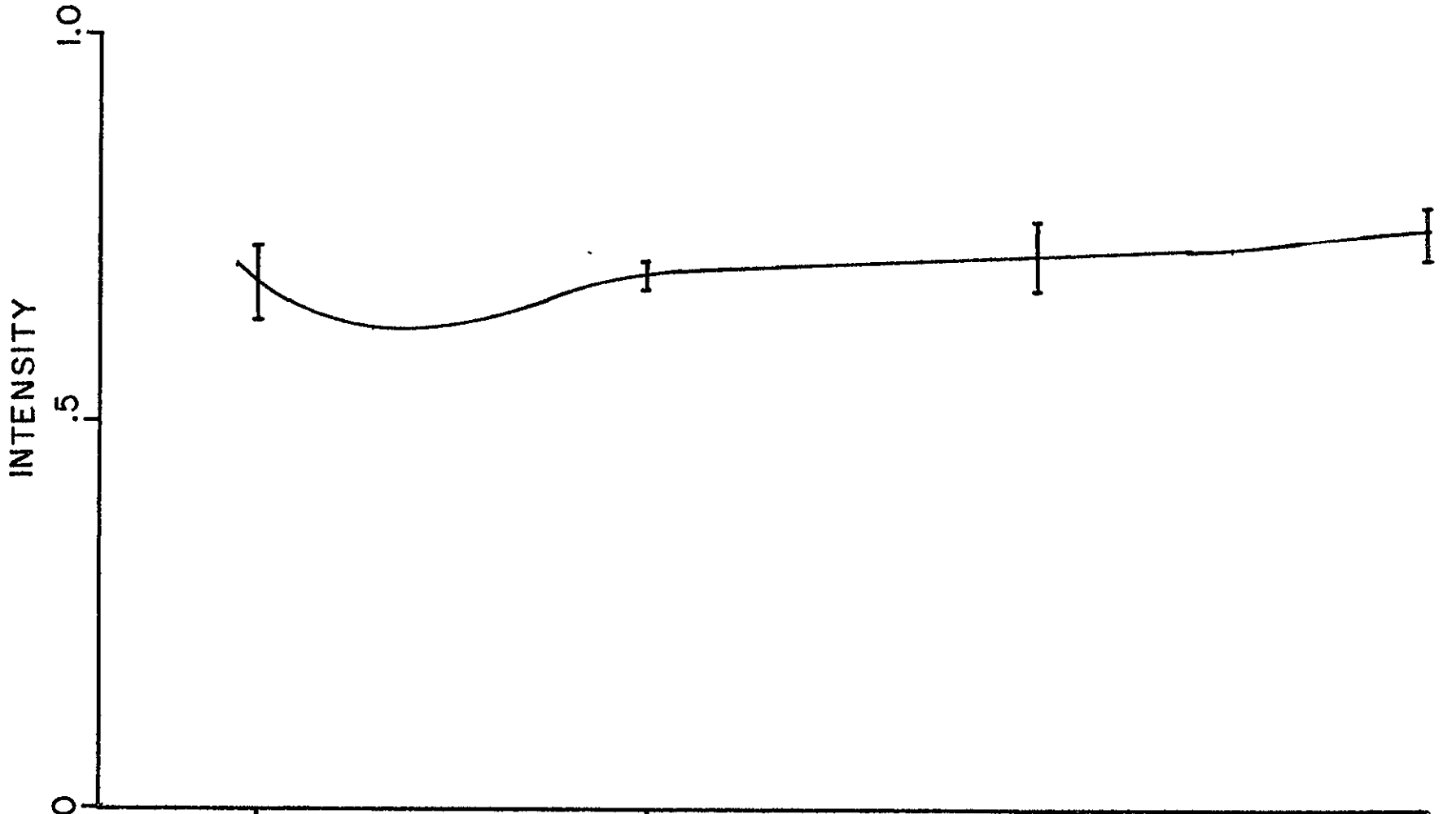

FIG. 8a

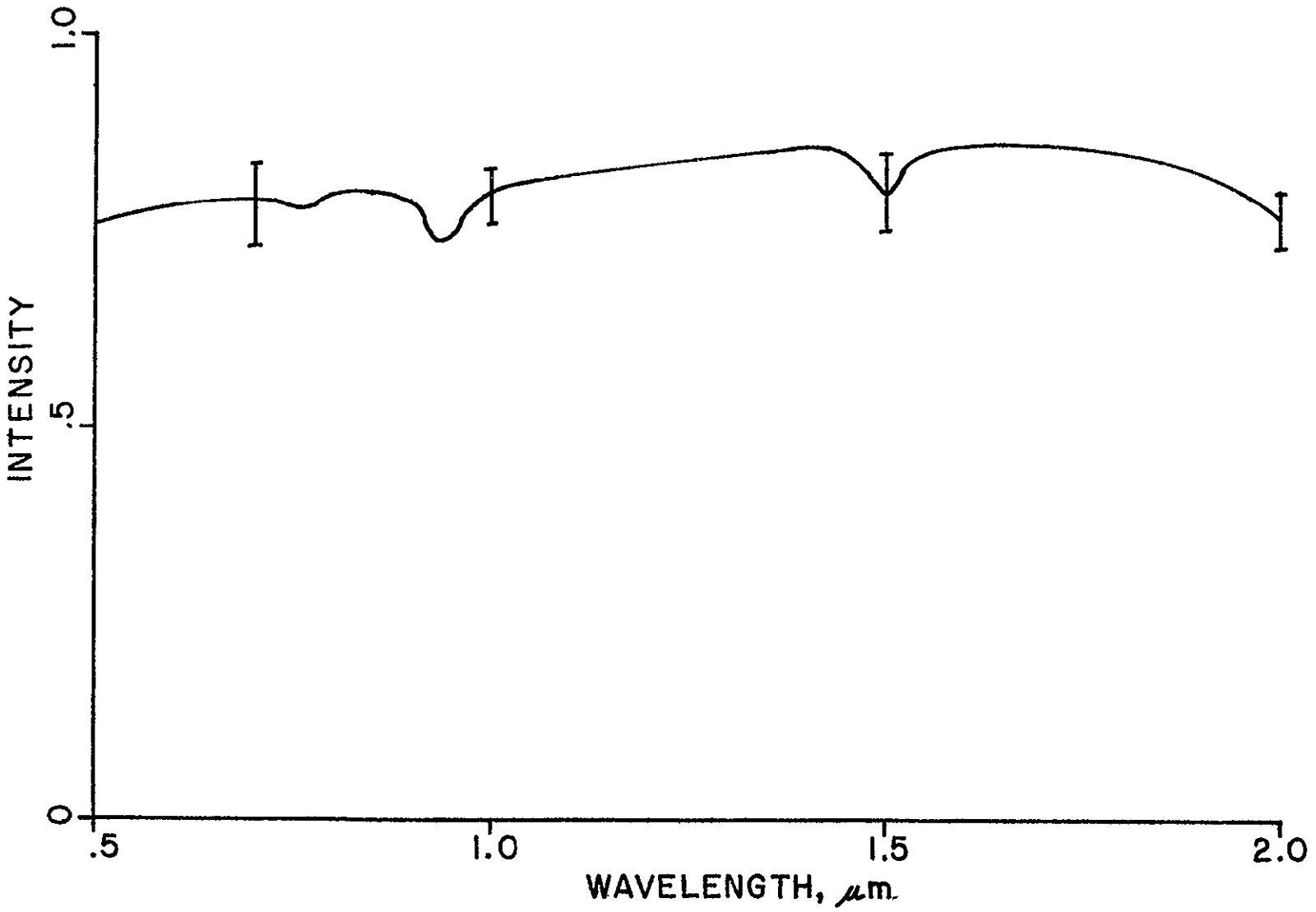

FIG. 8b

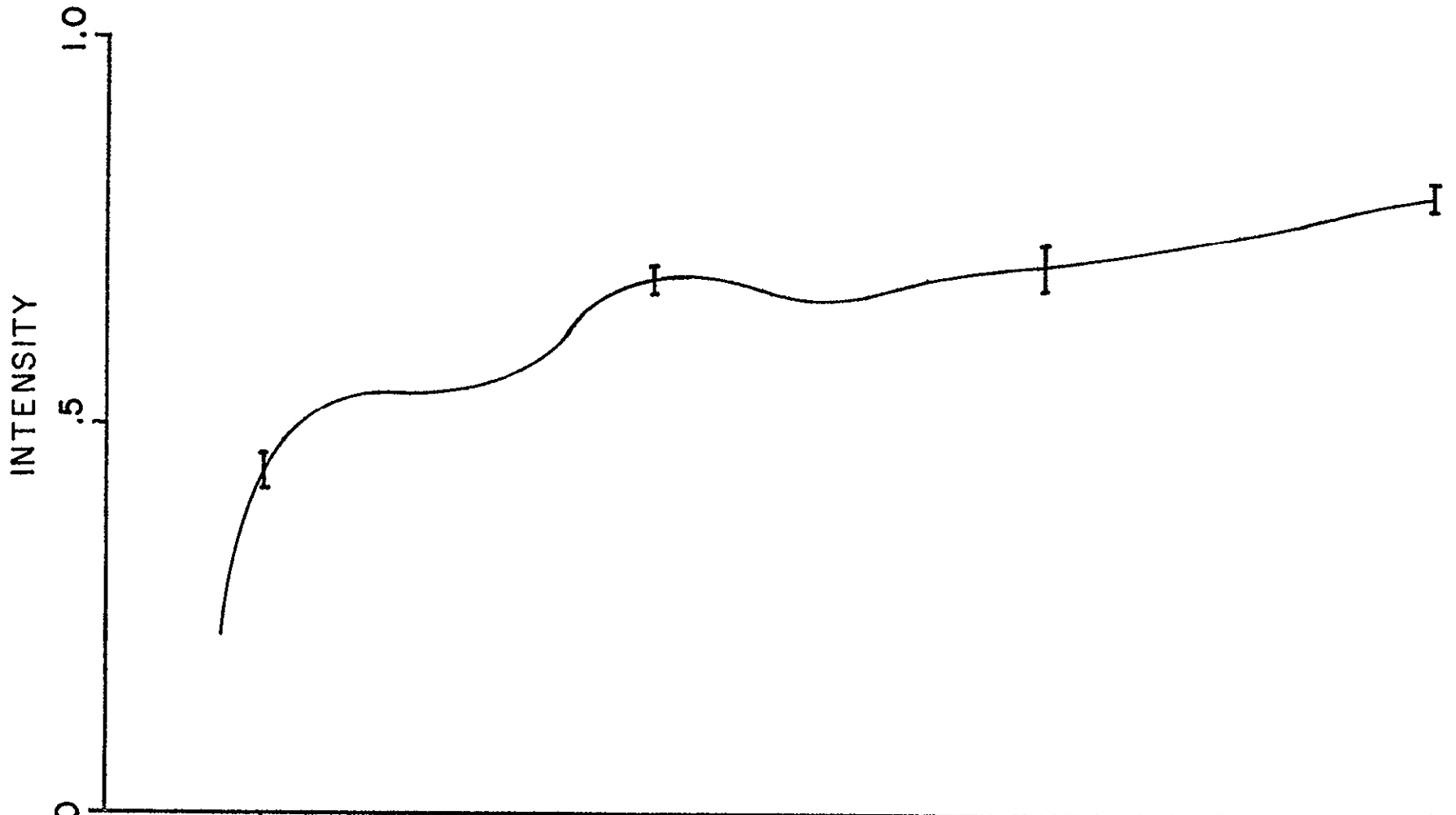

FIG. 9a

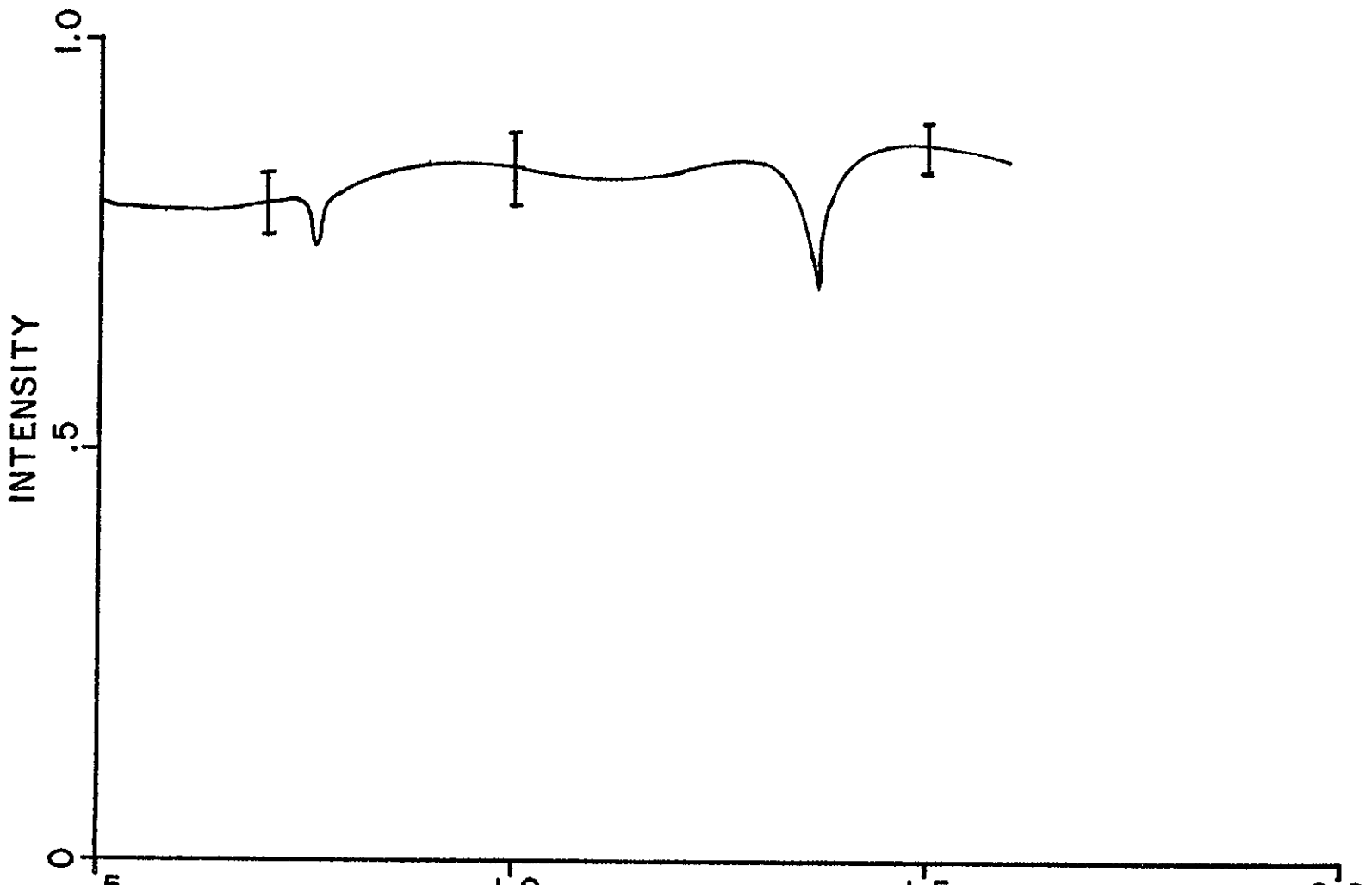

FIG. 9b

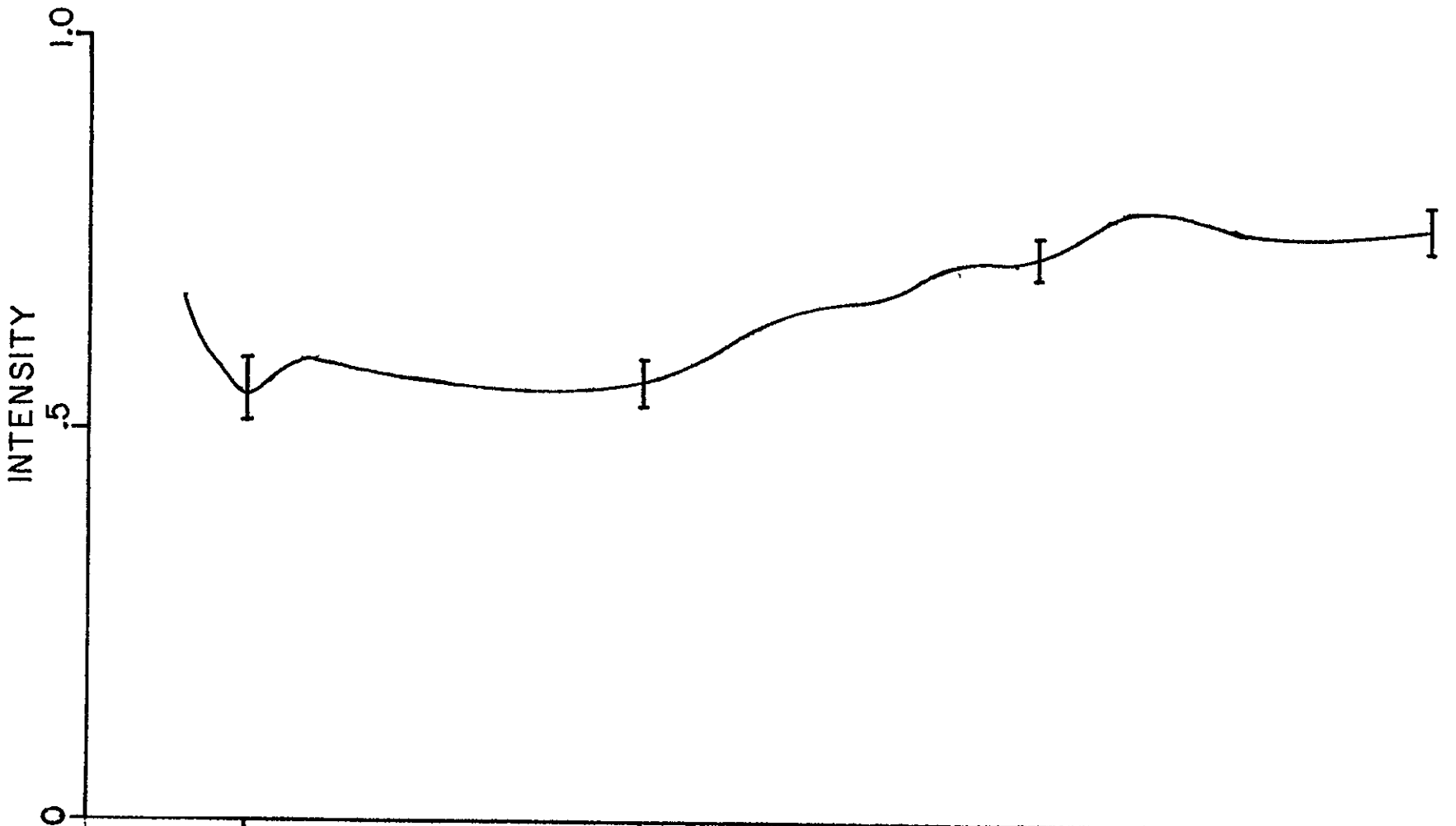

FIG. 10a

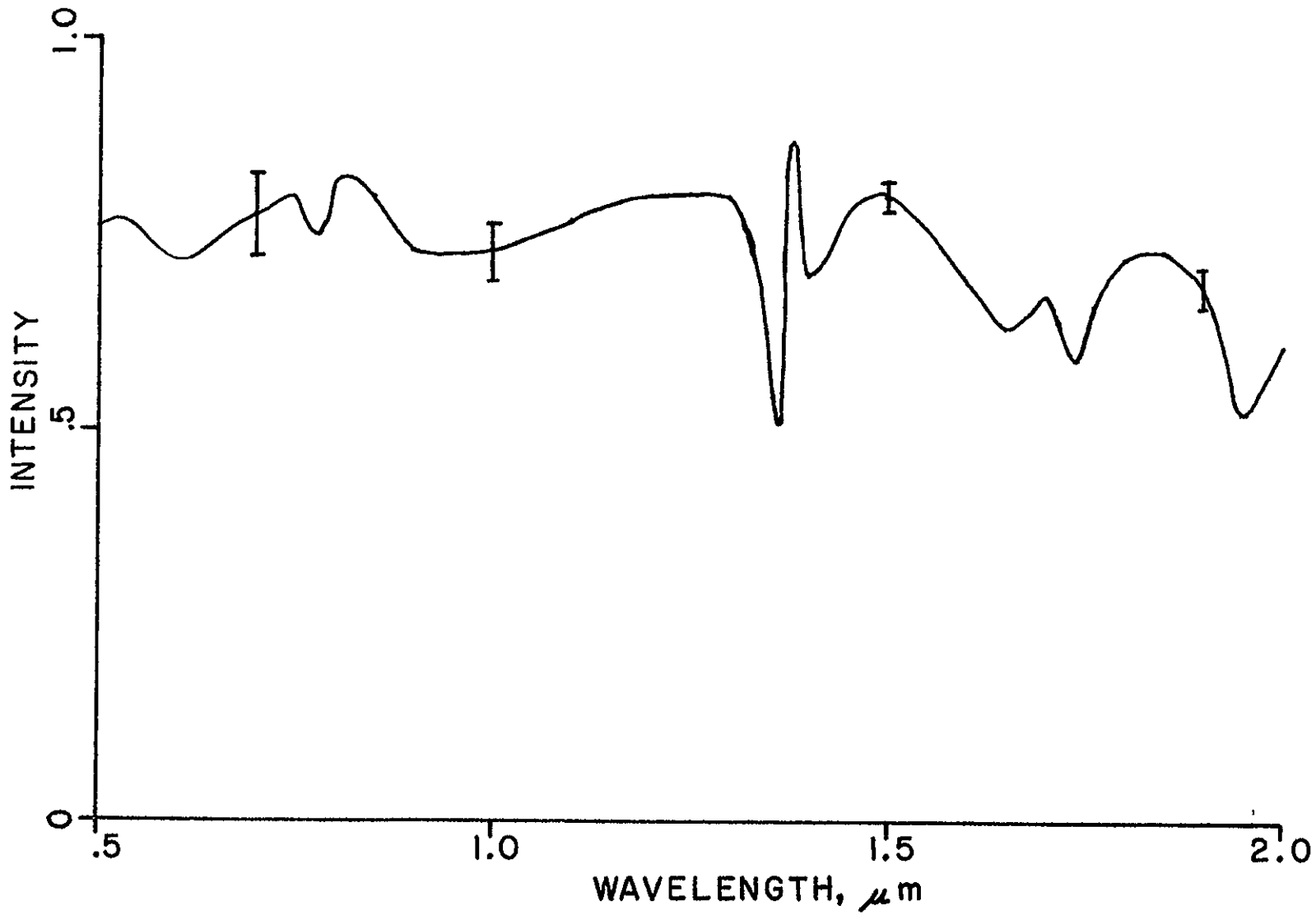

FIG.10b

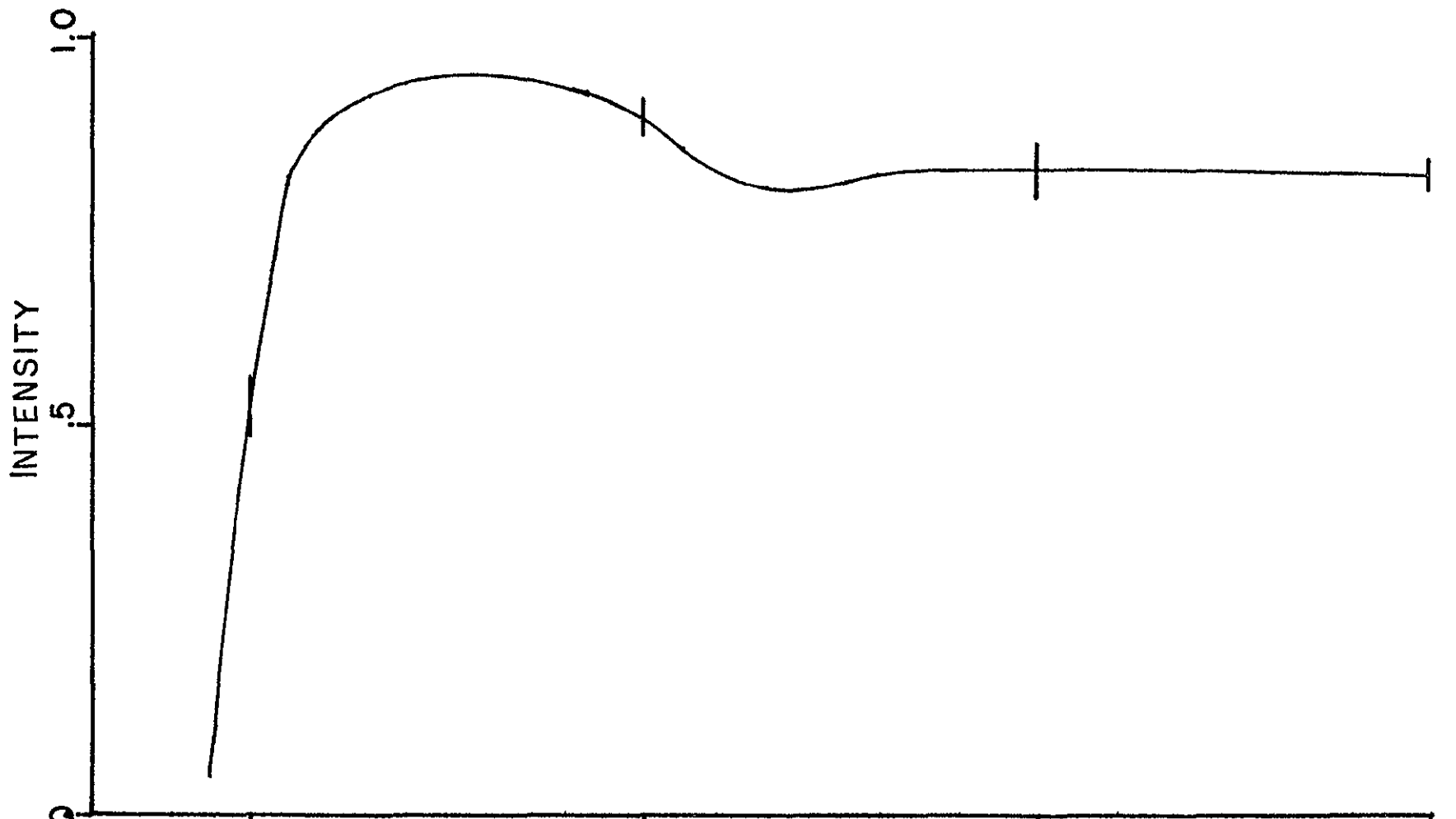

FIG. 11a

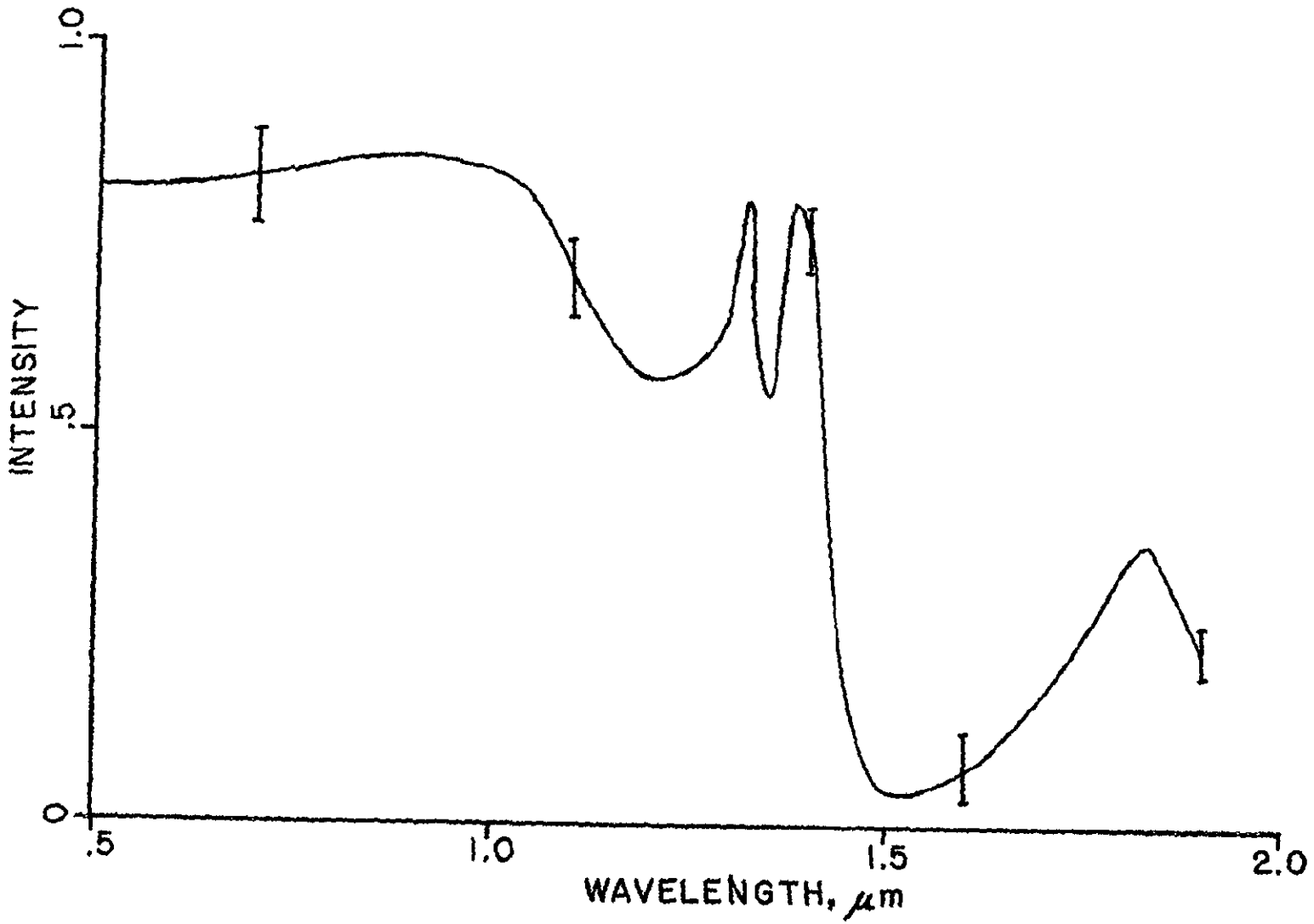

FIG.11b